Masterthesis

Surface Velocities in the Subpolar North Atlantic from Shipboard Observations and Satellite Altimetry

Robert Cordts

University of Bremen

rcordts@uni-bremen.de

Matrikel Nr. 2991929

1. Examiner: Dr. Christian Mertens

2. Examiner: Prof. Dr. Torsten Kanzow

August 17, 2017

Abstract

Satellite altimetry provides measurements of sea surface height which are processed to daily maps of absolute geostrophic surface velocity with a high geographic coverage at a spatial resolution of 0.25°. Here, satellite velocity data are compared to surface velocity measurements from shipboard acoustic Doppler current profiler (ADCP) in the subpolar North Atlantic (SPNA). An analysis of the data collected by RV Maria S. Merian in 2012 assesses different ways of averaging the full profiles measured by the ADCP with regard to their respective accordance with the velocities from satellite observations. The best accordance herein is found by applying a combined average over 2.5 h alongtrack and over depths from 46.5 m to 134.5 m. Subsequently, this averaging scheme is applied to ADCP measurements obtained during 15 individual research cruises in the SPNA in between 2003 and 2016. A statistical analysis of these shows that the velocity measurements are in agreement with correlation coefficients larger than 80% in both velocity components. Large root mean square (rms) deviations of roughly $11\,\mathrm{cm\,s^{-1}}$ between individual observations are persistent throughout the entire ensemble. These are mainly attributed to the large variance within averaged intervals of shipboard ADCP data on the one hand and ageostrophic features in the flow on the other, were the latter is physically plausible but not evident from the underlying data. Repeated measurements in different years along a zonal section at 47°N are used to average independent velocity measurements at identical locations; the rms deviations of the multi-annual averages dropped to roughly 50% of the initial values. Furthermore the satellite velocity observations are transferred to the subsurface transport within the upper 500 m. This transfer is established from the linear relation between ADCP transport measurements and satellite velocity measurements. A comparison of the direct shipboard observations to those calculated from the satellite data by means of the linear transfer function along 3 different sections gave a similar result as the comparison of velocities: A high correlation of $(84.3 \pm 7.1)\,\%$ of the in-situ transports and those calculated from altimetric velocities is accompanied by large rms deviations of $(4.4 \pm 1.1)\,\mathrm{Sv}$. Averaging all available transports within one section reduces the relative deviation of ADCP and satellite measurements to less than 13% for all three sections. Overall the findings indicate that the transfer function is not precise enough to infer information about the instantaneous subsurface flow from individual satellite measurements. However, averaged measurements show a striking accordance with the in-situ observations. Therefore a usage of e.g. monthly averages of the altimetric data could provide decent estimates of the subsurface transport.

Zusammenfassung

Satellitenaltimetrie ermöglicht Messungen der Höhe der Meeresoberfläche, aus welchen sich tägliche Karten absoluter geostrophischer Oberflächengeschwindigkeit bei hoher geographischer Abdeckung und einer räumlichen Auflösung von 0.25° ableiten lassen. In dieser Arbeit werden altimetrisch ermittelte Geschwindigkeiten mit den Beobachtungen von Ultraschall-Doppler-Profil-Strömungsmessern (ADCP) im subpolaren Nordatlantik verglichen. In Hinblick auf die Übereinstimmung mit den Satellitenmessungen werden verschiedene Mittelungsverfahren der per ADCP gemessenen Geschwindigkeitsprofile verglichen. Die beste Übereinstimmung ergibt sich hierbei für eine kombinierte Mittelung über 2.5 h entlang der Schiffsroute sowie über Tiefen von 46.5 m bis 134.5 m. Diese Mittelung wird auf die ADCP Messungen von 15 Forschungsfahrten im subpolaren Nordatlantik angewandt. Es zeigt sich, dass die gemittelten ADCP Daten weitgehend mit den Satellitenmessungen übereinstimmen, mit Korrelationen von über 80% in beiden Geschwindigkeitskomponenten. Die quadratisch gemittelten Abweichungen zwischen einzelnen Beobachtungen liegen bei etwa 11 $\mathrm{cm\,s^{-1}}$. Die Größe der Abweichungen zwischen den altimetrischen und den in situ gemessenen Geschwindigkeiten wird zum einen der großen Varianz zugerechnet, welche die Intervalle der ADCP Messungen, über die gemittelt wird, aufweisen sowie zum anderen ageostrophischen Anteilen in der Strömung. Letzteres ist physikalisch plausibel, geht jedoch nicht eindeutig aus den zugrunde liegenden Daten hervor. Die Mittelung wiederholter Messungen aus unterschiedlichen Jahren am selben Ort reduziert die quadratisch gemittelte Abweichung auf etwa 50% unterhalb jener der Ausgangsdaten. Des Weiteren wird über die lineare Beziehung von ADCP Transportmessungen in den oberen 500 m und per Satellitenaltimetrie gemessenen Oberflächengeschwindigkeiten eine Verknüpfung zwischen beiden hergestellt. Entlang dreier Schnitte wird ein Vergleich der per ADCP gemessenen Transporte mit den über die Transferfunktion aus den Satellitendaten abgeleiteten durchgeführt, welcher ähnliche Ergebnisse wie der Geschwindigkeitsvergleich liefert: Eine hohe Korrelation von $(84.3 \pm 7.1)\,\%$ zwischen den in situ gemessenen und den altimetrischen Transporten wird von einer quadratisch gemittelten Abweichung von $(4.4 \pm 1.1)\,\mathrm{Sv}$ begleitet. Die Mittelung aller Transporte, welche entlang eines bestimmtes Schnittes ermittelt wurden, reduziert die relativen Abweichungen zwischen ADCP und Satellitenmessungen auf unter 13%. Insgesamt deuten die Ergebnisse darauf hin, dass die Transferfunktion nicht präzise genug ist um aus einzelnen Satellitenmessungen Informationen über den momentanen Fluss unterhalb der Meeresoberfläche abzuleiten. Nichtsdestotrotz weisen die gemittelten Werte eine große Übereinstimmung mit den in situ Beobachtungen auf. Daher ließen sich etwa aus monatlichen Mitteln der Satellitendaten zuverlässige Abschätzungen des Transports unterhalb der Oberfläche berechnen.

Contents

1. Introduction

Physical oceanography is based on the intertwining of theory, observation and numerical modelling. Developing a theory that can grasp the complexity of a convecting, wind-forced turbulent fluid moving on a rotating sphere is an ongoing endeavour and far away from being able to predict features of the oceanic circulation prior to their observation. Hence the observation of the ocean continues to be important for its comprehension. However, while today the ocean is sampled to a degree that is unprecedented, the available in-situ data remains sparse in space and time, insufficient for understanding the ocean in all of it's variability (Stewart, 2008). On a fundamental level this under-sampling problem is caused by two different factors. On the one hand there is the ocean's opacity to electromagnetic radiation which makes is necessary to physically place an instrument at the location of a desired measurement (Wunsch and Stammer, 1998). On the other hand there is the vastness of the oceanic system, i.e. the volume of water that has to be sampled in relation to the speed and cost of conducting oceanographic in-situ observations.

The described under-sampling problem is closely related to ship-based data collection, which from the beginnings of the subject has been the elementary observation tool for oceanographic science. Since ship speed is limited, the larger the area that is to be observed gets, the longer the time that passes between the beginning and end of an observation becomes. A modern research vessel has a typical speed of about 12 kn. If it was to conduct measurements along a zonal section crossing the Atlantic, it would take weeks in between the first and last measurement – that is, without considering the time used for station measurements. Moreover, as mentioned before, the amount of ship-based observations that is feasible is limited by the their cost. For a global circulation that was constant over time or changing very slowly this modus operandi would be quite suitable (Wunsch and Stammer, 1998). However, it is a well-known fact that the ocean is constantly changing (e.g. Helland-Hansen and Nansen, 1920). Munk (2000) summarized this in a blunt statement: "If I were to choose a single phrase to characterize the first century of modern oceanography, it would be 'a century of undersampling'."

One solution which tackles this problem is the use of satellite altimetry which enables almost instantaneous sampling of the sea surface over large areas. The geostrophic surface velocity presents a parameter routinely measured by Earth-orbiting satellites (Tapley et al., 2003; Maximenko et al., 2009; Birol et al., 2005). For more than two decades satellites have been measuring the sea surface topography with great precision, accurate to about 3 cm relative to the center of the Earth (e.g. Chang et al., 2016; Talley et al., 2011). First enabled by the estimation of the Geoid through the GRACE mission (Tapley et al., 2004; Wunsch and Gaposchkin, 1980) and further advanced by the GOCE Geoid model (Rio and Hernandez, 2004; Rio et al., 2013) these measurements are not any longer relative to some satellite's height alone but can be made absolute. Today there are maps of absolute surface velocity, available at a daily resolution on a global grid as small as 0.25° x 0.25°. Satellite oceanography presents an essential component of operational oceanography[1] and satellite measured ocean variables such as the surface geostrophic velocity are of great importance to constrain ocean models and/or serve downstream applications (Traon et al., 2015). Today's common use of sea surface height (SSH) maps and the derived product has contributed to a much better understanding of the ocean's mesoscale dynamics (Le Traon, 2013).

This work is concerned with the comparison of satellite altimetric velocities to direct acoustic Doppler current profiler (ADCP) measurements within the subpolar North Atlantic (SPNA), using ADCP profiles acquired from 2003 to 2016. The question to which extent such velocity measurements obtained from remote sensing satellites are in agreement with in-situ observations has been carried out previously. In the following I will outline the numerous comparisons that exist between satellite altimeter derived geostrophic currents and in-situ velocity observations for different regions, SSH products and in-situ instruments. Due to a difference in one or several of these factors, some of the preceding findings will only be suitable for a qualitative comparison with this work's results while others allow for a quantitative comparison

Yu et al. (1995) found a correlation of 92% (zonal) and 76% (meridional) between co-located drifter and altimetric velocities in the western tropical Pacific in a comparison of satellite-tracked drogued surface drifters and geostrophic velocities derived from monthly maps of SSH.Kelly et al. (1998) found a similar correlation of 73% in the California Current comparing low-pass-filtered in-situ velocities to satellite measured geostrophic velocities. The in-situ

[1] Following the *European Global Ocean Observing System*, operational oceanography can be defined as the activity of systematic and long-term routine measurements of the seas, oceans and atmosphere, and their rapid interpretation and dissemination (*http://eurogoos.eu/about-eurogoos/what-is-operational-oceanography/*).

instruments in this case were World Ocean Circulation Experiment surface drifters and moored acoustic Doppler current profilers while the altimeter data was taken along subtracks of the TOPEX/POSEIDON mission. Kelly et al. (1998) furthermore found the component of the satellite velocities that was uncorrelated with the in-situ velocities to be in turn correlated with the wind-driven Ekman transport. In the same region, Strub et al. (1997) evaluated the temporal and horizontal resolution of geostrophic surface velocities calculated from TOPEX satellite altimeter heights in comparison with moored velocities from vector-averaging current meters and an ADCP at depths below the Ekman layer. They found the root-mean-square (rms) difference between the altimeter and current meters to be $7-8\,\mathrm{cm\,s^{-1}}$. Being relatively high compared to the signal size, a significant part of this value is attributed to small-scale variability. Zlotnicki et al. (1993) raised the question whether it is possible to measure the weak surface currents of the Cape Verde frontal zone by means of satellite altimetry and compared geostrophic velocities from Geosat SSH data to shallow current meter velocities. The correlation found in this comparison ranges from $32-90\%$ and exhibits a spatial dependency. When averaged over 30 days and 142 km, the rms error of the altimeter derived geostrophic current was found to stay below $2-3\,\mathrm{cm\,s^{-1}}$. A comparison in the equatorial Pacific region conducted by Picaut et al. (1990) showed that Geosat derived velocities and those from shallow current meter data are correlated by $50-80\%$ with a rms velocity difference varying from $15-30\,\mathrm{cm\,s^{-1}}$. In a summary of the above it can be stated that correlation coefficients between altimetric and in-situ velocity measurements are predominantly found to be ranging in between 50 and 90% (Ducet et al., 2000). The work of Ducet et al. (2000) itself only compares rms-altimeter-velocities to those from current meters and surface drifters in the North Atlantic, so despite falling in the region of interest, it doesn't provide any direct information as to which extent the actual velocities are in agreement. The work of Boebel and Barron (2003) is focused on the Agulhas Retroflection region. The comparison is made between MODAS-2D[2] fields of geostrophic velocity on the one hand and velocities from shipboard ADCP data as well as from neutrally buoyant RAFOS (Ranging and Fixing Of Sound) floats at intermediate depth on the other hand. They found a correlation of $80-90\%$ between the altimeter derived and the in-situ measured

[2]MODAS (Modular Ocean Data Assimilation System) provides an SSH product geo-referenced to a long-term SSH mean. By adding climatological SSH fields to provide space-time interpolated absolute steric SSH fields, MODAS should theoretically provide realistic geostrophic surface velocities and be able to reproduce quasi-permanent features of the flow such as western boundary currents or free jets (Boebel and Barron, 2003).

velocities with an error smaller than 5%. The rms deviation between the velocities from the various data sources was found to be $20-30\,\mathrm{cm\,s^{-1}}$. A linear regression between MOADS and RAFOS/ADCP velocities taken at different depths indicates that the in-situ velocities match the altimetric ones at the surface but significantly decrease with depth. This was inferred from the regression's slope between the different instruments' data being 1 at the surface and decreasing to 0.4 at depths below 1000 m. Boebel and Barron (2003) attribute this behaviour to the baroclinic velocity shear.

More recent and therefore assimilating the advancements in satellite altimeter products gained from the GRACE mission and the GOCE Geoid model is the study of Ohashi et al. (2013) in the Northwest Atlantic. They reconstruct the near-surface currents from multi-sensor satellite data by incorporating wind-induced Ekman currents and surface wave-induced Stokes drift which they calculate from scatterometer-measured wind velocities; on the Newfoundland and southern Labrador Shelves the reconstruction furthermore takes model-simulated currents into account. These composite currents show a fair agreement with instantaneous velocity measurements from shipboard ADCP data, as the two are correlated by 59%. Ohashi et al. (2013) found the absolute differences between the two instrument's observations to be rather large relative to the measured speeds. Based on the discrepancy between a correlation of 0.59 and absolute deviations which imply low accordance they suggest that forcings not included in the composite current, such as wind variability on small temporal and spatial scales significantly influence the order-of-days circulation variability in this region. However, the composite currents' mean speed at the sea surface is very similar to the one measured by the drifters, being $35\,\mathrm{cm\,s^{-1}}$ (composite current) and $35\,\mathrm{cm\,s^{-1}}$ (drifter), respectively.

Equally incorporating the newer generation Geoid model is the study of Pascual et al. (2009) which assesses the quality of real-time altimeter products. Making use of the same altimeter product that is also used in this work, their work compares the satellite data processed and distributed by AVISO (Archiving, Validation and Interpretation of Satellite Oceanographic data) to measurements obtained from Argos-tracked drifters with a drogue located at 15 m depth. The drifter velocities are obtained by time differencing processed 6-hourly positions and hence present a low-passed time series of the actual velocities. The comparison to the absolute velocity fields derived from the altimeter data is then accomplished by interpolating the mapped AVISO

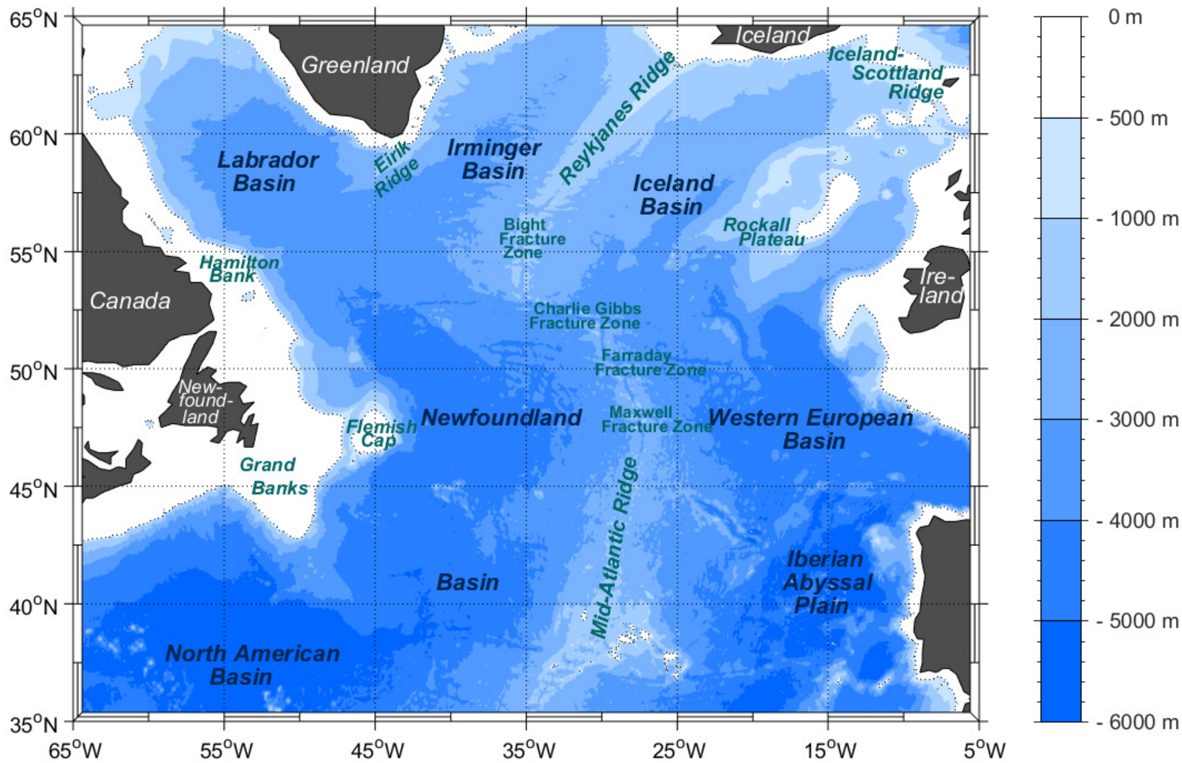

Figure 1: Bathymetric map of the subpolar North Atlantic with names of selected topographical features. The dotted contour indicates the -500 m isobath. The bottom topography is taken from the ETOPO2 database (U.S. Department of Commerce, 2001).

velocities onto the position and time of the drifter data, a method identical to the one adopted in this work. Therefore the rms differences between the AVISO velocities and those obtained from the drifter measurements as calculated by Pascual et al. (2009) are suitable for a direct comparison. Focusing on energetic zones with rms velocities larger than $20\,\mathrm{cm\,s^{-1}}$ that are deeper than 1000 m and outside of the equatorial band, the rms deviations between satellite and in-situ data were found to be $10.72\,\mathrm{cm\,s^{-1}}$ in the zonal and $9.97\,\mathrm{cm\,s^{-1}}$ in the meridional component, respectively. When given in percent of the drifter variance, this corresponds to a mean square difference between drifter and altimeter velocities of 24.3% (zonal) and 28.4% (meridional).

The way of addressing the question to what extent satellite altimetric velocity measurements compare to in-situ velocity observations will mainly depend on 3 factors (Boebel and Barron, 2003):

- What is the region of interest and which large scale-currents are of importance therein?
- What is the source of the velocity measurements on both sides, i.e. which satellite product is compared to which in-situ instrument?
- Finally, which physical parameters are considered and how is the accordance between the two instruments quantified?

In the following these three aspects will be looked at, providing for an approach towards answering the initial question. A brief description of the SPNA is given as the geographic region of interest. Thereafter an outline of the approach chosen in this work will elaborate how shipboard ADCP observations are compared to maps of absolute geostrophic surface velocity whereby their accordance will mainly be quantified by the root mean square deviation and correlation coefficient of the two instruments' data.

The geographical background of this work is the SPNA, located in between roughly 40°N and 60°N. Within the ocean it presents a climate relevant key region, playing a major role in the Atlantic meridional overturning circulation (e.g. Rhein et al., 2011). The basin-scale circulation in the SPNA is constituted of the Labrador Current carrying cold and fresh water towards the equator and the Gulf Stream and North Atlantic Current (NAC) carrying warm and saline water towards the Arctic (e.g. Mertens et al., 2014). The NAC is split into several branches after passing the Flemish Cap, forming current bands, eddies and meanders to eventually cross the Mid-Atlantic Ridge and enter the eastern Atlantic (Fig. 1). The westward recirculation of these water masses then forms the anticyclonic subpolar gyre. The circulation in the SPNA is characterized by dynamic features and large variability (e.g. Fratantoni, 2001), which allows the observation of large current velocities as well as fast changes of these.

The approach chosen in this work is divided into 3 parts as follows: To begin with, the velocity profiles collected along the cruise track of RV Maria S. Merian 21/2 in June and July 2012 are analysed in respect of their accordance with state-of-the-art velocity maps processed and distributed by AVISO[3]. This is done in order to test different ways of processing the ADCP

[3]The altimeter product used in this work was produced by SSALTO/DUACS (Segment Sol multimissions d'ALTimétrie, d'Orbitographie et de localisation précise/Data Unification and Altimeter Combination System) and distributed by AVISO, with support from CNES (Centre National d'Etudes Spatiales) – *http://www.aviso.altimetry.fr/duacs/*.

data, in particular concerning the averaging in time and space as well as tidal correction.

Secondly, using the results from this comparison, a consistent way of processing the high resolution ADCP profiles is applied to the data collected along 15 research cruises in the SPNA in between 2003 and 2016. This allows for the comparison of a large ensemble of velocity measurement pairs taken by the shipboard ADCP on the one hand and the AVISO satellite data on the other hand. A statistical analysis based on this large pool of data is to answer the following questions:

- How large is the absolute deviation between a velocity measurement taken by means of ADCP just below the surface and one obtained directly at the surface via satellite altimetry?
- How correlated are two such measurements?
- Do these parameters of accordance vary significantly between cruises conducted in different years?
- Do they vary spatially across the domain considered?

It will be seen that the analysis allows for an explanatory approach about what cause the differences that are found. They will at least partly be attributed to the comparative method.

Thereafter, the third and last part takes the relation between the 2 data sets a step further in showing that the satellite measured geostrophic surface velocity can be correlated with the transport in the upper ocean layer, specifically the layer in between 50 m and 550 m depth, measured by the shipboard ADCP. A transfer function is set up, utilizing the empirical linear relation to link the 2 quantities. This concept is subsequently tested on 3 different sections in the SPNA, i.e. the transport across the section as measured by the ADCP profiles is directly compared to that calculated from satellite altimetric velocities via the linear transfer function. This part of the work is focused on the following questions:

- How well is the transport in the upper ocean layer correlated with absolute geostrophic surface velocities?
- Is it possible to utilize the satellite data for gaining information about the volumetric transport below the surface? If so, to which extent can this empiric relation be used?

As a last point the transport across the mentioned sections is calculated from the daily maps of

AVISO velocities. This results in 3 transport time series with a daily resolution given for the time from 1993 to 2016.

The very last part of this work demonstrates why the approach chosen is so appealing: Linking two different ways of measuring the same physical quantity, namely the velocity at the sea surface is driven by the wish to combine the different positive aspects found in both. If it is possible to combine the high resolution depth profiles of velocity measured by the ADCP with the spatial and temporal coverage of remote sensing satellites, it may be feasible to obtain transport time series with a daily resolution from the satellite altimeter data.

2.1. Satellite Altimetry

Satellite altimetry describes the remote sensing of the SSH with a radar altimeter (Fig. 2). The altimeter emits radar pulses and records the runtime of the echo that is reflected to the radar antenna from the Earth's surface. Given sufficient knowledge about the pulse's propagation velocity in the atmosphere the distance between the sensed surface and the satellite is calculated. This distance is referred to as range (R). The position of the satellite is also determined with respect to an Earth-fixed frame of reference. This arbitrary reference ellipsoid roughly approximates the Earth's surface shape, it's origin is the Earth's center of mass.[4] If the satellite's height above the reference ellipsoid is denoted by S, subtracting the range yields the desired sea surface height:

$$\mathrm{SSH} = S - R \tag{1}$$

The SSH can be seen as the sum of two constituents, the geoid and the absolute dynamic topography (ADT):

$$\mathrm{SSH} = \mathrm{geoid} + \mathrm{ADT} \tag{2}$$

The geoid is the hypothetical height of the sea surface in the absence of any perturbations such as tides, wind stress and ocean currents. It is an equipotential surface whose height varies due to horizontal variations in the Earth's gravity field; these in turn are caused by density differences below the seafloor as well as by the ocean bottom topography. ADT is defined as the sea surface height with respect to the geoid. It comprises both a stationary component referred to as mean dynamic topography (MDT) and a highly variable component referred to as sea level anomaly (SLA):

$$\mathrm{ADT} = \mathrm{MDT} + \mathrm{SLA} \tag{3}$$

The MDT is linked to the circulation that is quasi-constant over time, induced by quasi-stationary forcing such as averaged wind fields. The SLA on the other hand includes variable features produced for instance by seasonal changes in wind or evaporation and precipitation patterns. It is computed by subtracting a long-term mean of SSH measurements referred to as mean sea surface (MSS) from the SSH itself:

[4]There are different ways to track the satellite's position; Topex/Poseidon is equipped with the Doris system, information on whose principle can be found via the AVISO homepage *http://www.aviso.altimetry.fr/en/techniques/doris/principle.html*.

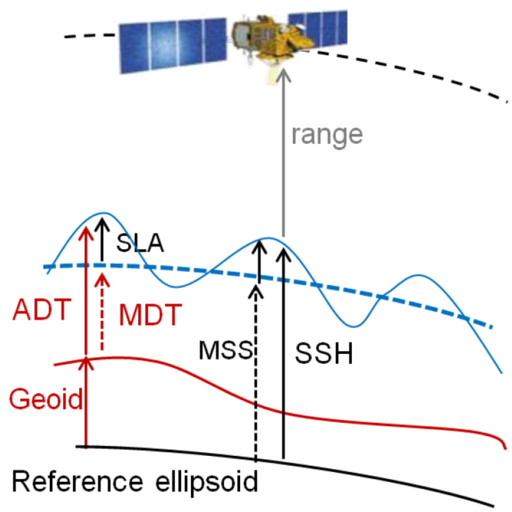

Figure 2: Naming convention for different reference layers used in satellite altimetry: Sea Surface Height = SSH, Mean Sea Surface = MSS, Mean Dynamic Topography = MDT, Absolute Dynamic Topography = ADT, Sea Level Anomaly = SLA (SSALTO/Duacs new product version, 2014).

$$\mathrm{SLA} = \mathrm{SSH} - \mathrm{MSS} \tag{4}$$

From Eqn. 2 the ADT can be directly inferred by subtracting the geoid from the altimetric SSH measurements if the former is known with sufficient accuracy. In practice, the satellite product used in this work utilises the MDT as a reference surface (SSALTO/Duacs new product version, 2014), such that

$$\mathrm{ADT} = \mathrm{MDT} + \mathrm{SLA} = \mathrm{MDT} + \mathrm{SSH} - \mathrm{MSS}, \tag{5}$$

in which a high resolution MDT is calculated as decribed by Rio et al. (2013). While this MDT does take into account the geoid model generated from the 4^{th} generation GOCE direct solution gravity field model (GOCE DIR-R4), it also assimilates in-situ hydrographic observations from ARGO floats and drifting buoys velocities in a multivariate objective analysis.

2.2. Geostrophic Balance

Geostrophy describes a flow in which horizontal Coriolis acceleration and horizontal pressure gradient force balance each other, while vertically the flow is in hydrostatic balance, i.e. the vertical pressure gradient force balances gravity.[5] This results in a flow that is not accelerated

[5] The basic theory of geostrophic balance that is layed out in the following is well described both in Talley et al. (2011) and Stewart (2008).

and is perpendicular to both the pressure gradient- and Coriolis force. All motion therefore occurs parallel to isobars in a horizontal plane. The horizontal force balance can be expressed in terms of geostrophic velocity (u_g,v_g),

$$u_\mathrm{g} = -\frac{1}{f\rho} \cdot \frac{\partial \mathrm{p}}{\partial y} \tag{6}$$

$$v_\mathrm{g} = \frac{1}{f\rho} \cdot \frac{\partial \mathrm{p}}{\partial x} \tag{7}$$

where ρ is the density of seawater, g is the gravitational acceleration, $f = 2\,\Omega \sin(\phi)$ is the Coriolis parameter at latitude ϕ, Ω is the period of the Earth's rotation about its own axis and $\partial p/\partial x$ and $\partial p/\partial y$ are the horizontal pressure gradient in zonal and meridional direction, respectively.

For a flow to be geostrophic, both viscosity and the nonlinear terms in the equation of motion need to be negligible compared to the Coriolis and pressure gradient acceleration. This generally presents a good approximation for the large scale flow within the ocean's interior, i.e. outside the top and bottom Ekman layers. Large scale in this case refers to distances over roughly 50 km and temporal scales greater than several days, hereafter summarized as the *synoptic* scale.[6]

In the ocean the horizontal pressure gradient is determined by the spatial distribution of density. At one specific depth the pressure below a point of high sea surface is larger than below a point of low sea suface, that is always with respect to the geoid. Hence, the horizontal pressure gradient force is generally acting from below high sea surfaces towards below low sea surfaces. One can therefore replace the pressure gradient in Eqn. 6 and 7 by the gradient of the sea surface height η to get the geostrophic velocity at the sea surface:

$$u_\mathrm{g} = -\frac{g}{f} \cdot \frac{\partial \eta}{\partial y} \tag{8}$$

$$v_\mathrm{g} = \frac{g}{f} \cdot \frac{\partial \eta}{\partial x} \tag{9}$$

Therefore it is possible to use maps of ADT to extract maps of the absolute geostrophic currents. Here, such maps are used, which are processed and distributed by AVISO. They are based on the all-satellite merged ADT, which at any given time combines SSH measurements from at least 2 and up to 4 satellite missions among HaiYang-2A, Saral/AltiKa, Cryosat-2, Jason-1,

[6]Stewart (2008, p. 152) gives a thorough scale analysis justifying the geostrophic balance that would exceed the scope of this work.

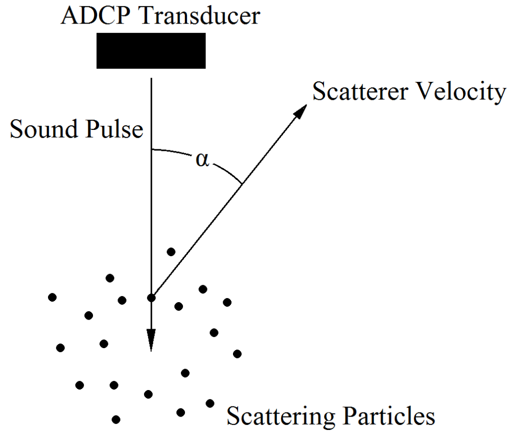

Figure 3: Scattering geometry of an ADCP measurement. Modified from *TRD* Broadband Primer (2006).

Jason-2, T/P, Envisat, Geosat-Follow-On and ERS-1/-2 (SSALTO/Duacs User Handbook, 2016). While the individual satellites have a repeat cycle between 10 and 35 days, the mapped product is interpolated to a temporal resolution of 1 day. It is given with a spatial resolution of 0.25° x 0.25° on a cartesian grid. Details on the mapping process are given in Arbic et al. (2012). In following these velocities are referred to as satellite or AVISO velocities.

2.3. Measuring Ocean Currents with an Acoustic Doppler Current Profiler

The acoustic Doppler current profiler (ADCP) provides a method for measuring the velocity of the water in range of the instrument. Its working principle is based on the fundamental assumption that on average small particles and plankton move passively with the same direction and speed as the water they are suspended in. The instrument emits a sound wave whose Doppler shift in frequency can be measured to infer the relative motion between the scattering particles and the instrument.

The Doppler effect describes a change in sound pitch that occurs for an observer moving relative to the source of sound. If the receiver and the sound source move at velocities v_r and v_s with respect to the same medium and directly approach or recede from each other, the relation between emitted frequency f_0 and observed frequency f_1 is given by

$$f_1 = \frac{c + v_\mathrm{r}}{c + v_\mathrm{s}} \cdot f_0 \tag{10}$$

in which c denotes the speed of sound; v_r is positive and v_s is negative for source and receiver approaching each other. If both v_r and v_s are small compared to c, this reduces to

$$\Delta f = \frac{\Delta v}{c} \cdot f_0 \tag{11}$$

where $\Delta f = f_1 - f_0$ is the observed change in frequency and $\Delta v = v_r - v_s$ is the relative velocity between source and observer. This limiting case of Eqn. 10 generally holds for oceanographic velocities which are several orders of magnitude smaller than the speed of sound in water. Since both the wave absorbed by the particles and the wave reflected back to the ADCP are affected by the Doppler shift, the Δf described in Eqn. 11 doubles. Moreover, if the ADCP transducer and the scatterers are allowed to move at an angle α relative to each other, Δf reduces with $\cos(\alpha)$ (Fig. 3). This yields the actual observed change in frequency

$$\Delta f = 2\frac{\Delta v}{c} \cdot f_0 \cdot \cos(\alpha) \tag{12}$$

An ADCP mounted to the ship's hull for operation along the ship's path is referred to as vessel mounted or shipboard ADCP. This work utilises shipboard ADCP data recorded during 15 individual cruises in between 2003 and 2016 covering different, to a large extent overlapping parts of the western subpolar North Atlantic (Tab. 1, Fig. 5). For all of these the instrument on board was a *TRD Instruments* Ocean Surveyor operating at 75 kHz[7]. It uses a flat phased-array transducer which was configured to collect narrow bandwidth water-profile data. The data were recorded into depth bins varying between 4 m and 16 m for individual cruises. The ADCP can be operated either in long range mode or high precision mode. The maximum range varies between 410 m and 822 m for the different data sets depending both on the choice of operational mode and vertical resolution cell size. The raw data have a temporal resolution of about 0.7 Hz which reflects the rate at which the instrument can transmit and process it's pulses. The velocity profiles dealt with in this work have already been averaged into 1 min ensembles for all cruises except the MSM5/1 and the MET59/2 cruise, in which case the profiles were averaged into 2 min and 4 min ensembles, respectively.

2.4. Averaging of ADCP Data and Interpolation of AVISO data

The main objective is to average all ADCP profiles into a timeseries $\vec{u}(\vec{x}, t)$ that most closely matches the AVISO velocities at the respective time and space. Three different methods of averaging are tested based on the data recorded along the cruise 21/2 of RV Maria S. Merian

[7]The 75 kHz shipboard ADCP has a higher spatial resolution than the 38 kHz ADCP at the cost of a smaller range. So even though its data would have equally been available from the cruises listed above, they were not used since the main interest here is in the velocity close to the surface. The larger range of the 38 kHz ADCP is of no advantage given the depth interval of interest in this work.

Cruise Name	Day / Month	Year	Cell Size	Range	Abbrev.
Meteor 59/1	29 June - 19 July	2003	8 m	22 m to 814 m	MET59/1
Meteor 59/2	23 July - 29 August	2003	8 m	22 m to 814 m	MET59/2
Thalassa SPOL	4 June - 12 July	2005	16 m	22 m to 806 m	ThalSP
M.S.Merian 5/1	14 April - 3 May	2007	16 m	38 m to 822 m	MSM5/1
M.S.Merian 9/1	23 July - 18 August	2008	16 m	32 m to 822 m	MSM9/1
M.S.Merian 12/3	15 July - 4 August	2009	8 m	32 m to 822 m	MSM12/3
Meteor 85/1	24 June - 02 August	2011	8 m	18 m to 810 m	MET85/1
M.S.Merian 21/2	25 June - 24 July	2012	8 m	18 m to 810 m	MSM21/2
M.S.Merian 27	19 April - 6 May	2013	4 m	14 m to 410 m	MSM27
M.S.Merian 28	9 May - 20 June	2013	8 m	18 m to 810 m	MSM28
M.S.Merian 38	7 May - 5 June	2014	8 m	18 m to 810 m	MSM38
M.S.Merian 39	8 June - 2 July	2014	8 m	18 m to 810 m	MSM39
M.S.Merian 42	2 May - 22 May	2015	8 m	22 m to 814 m	MSM42
M.S.Merian 43	25 May - 27 June	2015	8 m	22 m to 814 m	MSM43
M.S.Merian 53	31 March - 9 May	2016	8 m	22 m to 814 m	MSM53

Table 1: List of cruises whose shipboard ADCP data has been used. The column *cell size* refers to the vertical resolution cell size, i.e. the size of the depth bins that data are recorded into. The maximum range as given above can differ from the actual range, which depends a.o. on ship speed. Notably on 14 cruises, that is on all except M.S. Merian 27, measurements were taken below 550 m. In the following the cruises will be referred to by their respective abbreviation as given in the column to the right.

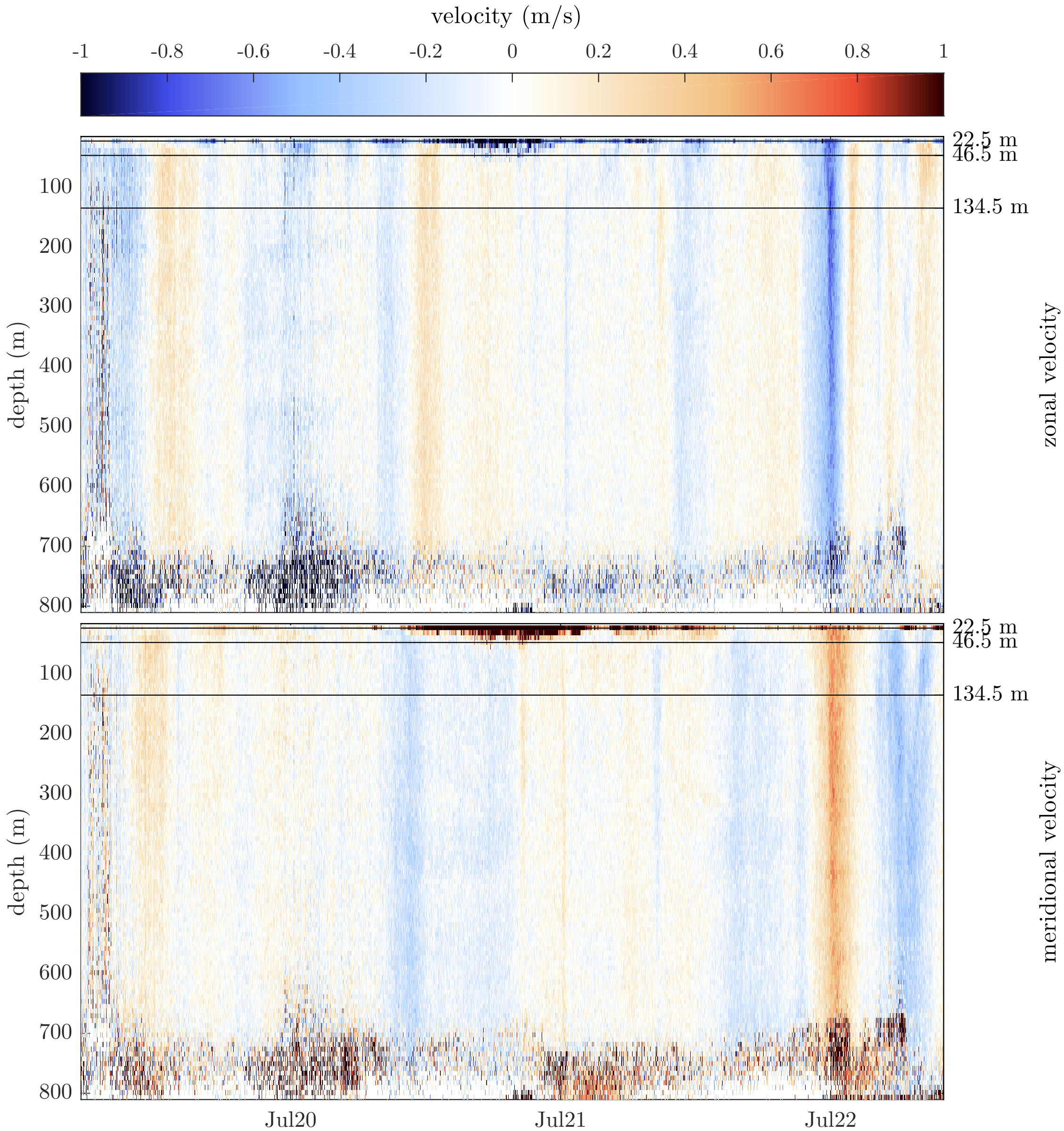

Figure 4: Profiles of zonal (upper panel) and meridional (lower panel) velocity, measured by shipboard ADCP along the cruise 21/2 of RV Maria S. Merian in July 2012; both panels show data that has been averaged into 1 min ensembles; the color scale is inclusive in both directions, i.e. the dark areas include all speeds exceeding $1\,\mathrm{m\,s^{-1}}$; black lines at depth levels 22.5 m, 46.5 m and 134.5 m indicate the 2 layers used for comparison with the satellite data; bins shallower than 50 m as well as the ones close to the range of the instrument are characterized by unreasonable velocities, exceeding speeds of $5\,\mathrm{m\,s^{-1}}$.

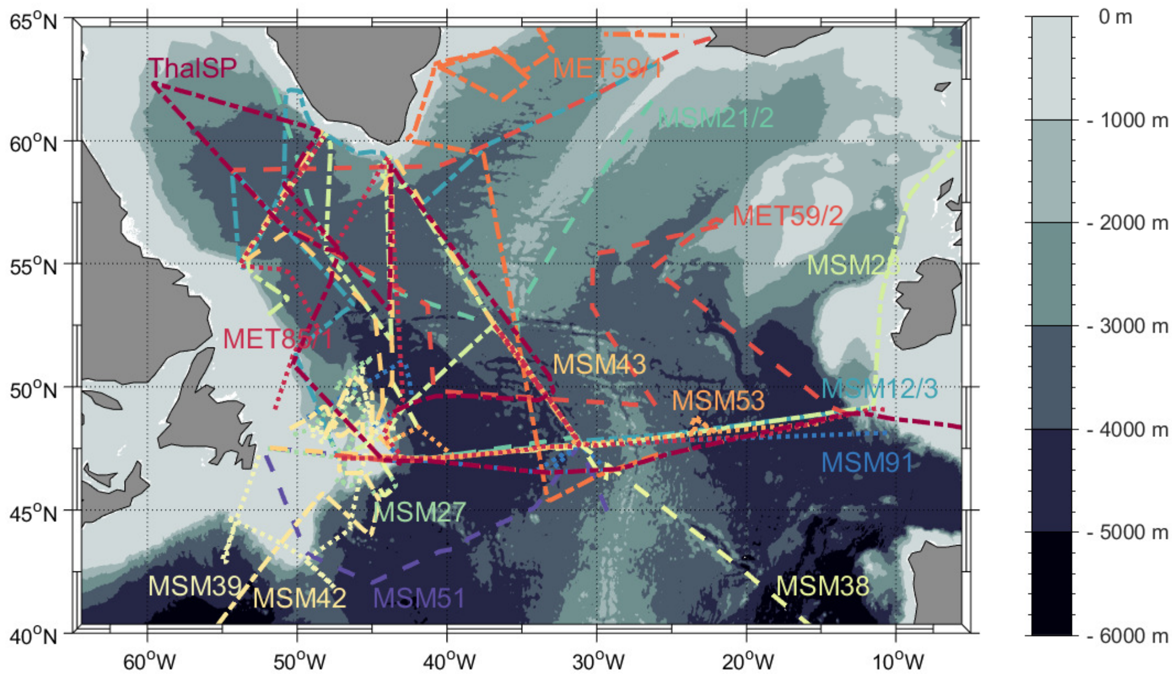

Figure 5: Cruisetracks of all cruises whose shipboard ADCP data has been used. Different cruise tracks may be covering identical or similar sections.

(MSM21/2) in June and July 2012 (Fig. 5). They differ both in the depth range that is considered and in whether the profiles are averaged into bins of constant time or fixed spatial width along the cruise track. In comparing various possibilities of processing the ADCP data, it is to be determined which one yields the best comparability with satellite measured surface velocities and shall hence be applied to all data sets listed in Tab. 1. Besides averaging the high resolution velocity profiles, the processing includes omitting bad data and removing tidal velocities, as outlined in the following. It is assumed that the results obtained from the analysis of the MSM21/2 cruise are applicable to the data from all cruises, since all ADCP observations were made with the same instrument and within a limited geographical region.

For a single-ping measurement to be accepted by the instrument, it needs to pass various error thresholds monitored by the ADCP. The *percent-good* (PG) parameter for each individual velocity bin is the percentage of pings that pass these criteria, which are large error velocity, low correlation and fish detection. Neglecting velocities with a low PG value therefore increases the quality of the remaining data, though in practice the effect is usually small (Thomson and Emery, 2014). The PG threshold below which data are omitted indeed showed to have no significant influence on the accordance of ADCP and AVISO data. Therefore this threshold presents an arbitrary measure and was set to 80 %, which left more than 98 % of the data to be used in the depth range of interest.

To calculate a value that most closely represents geostrophic velocity at the surface, the given depth profiles with their high temporal resolution need to be averaged both in depth and along the cruise track, i.e. in space and time. In search of an averaging scheme that does this while at the same time maximizing the accordance between ADCP and AVISO data three different averages were compared. The first one calculates an arithmetic average over 2.5 h and depth bin 5 to 15, corresponding to depths from 46.5 m to 134.5 m. By experience this depth range provides for a reference layer with little to no bad or missing values (Hummon and Firing, 2003). On the contrary, the bins above this layer are generally characterized by a smaller amount of valid data (Fig. 4); moreover surface effects such as wind induced motion are superimposed onto the synoptic scale flow at and close to the surface. Nevertheless a second average uses the same window of 2.5 h but considers only bin 2 to 4, equivalent to depths from 22.5 m to 46.5 m because the satellite measures directly at the surface. In the following this upper layer (22.5 m to 46.5 m) is referred to as surface layer. The very first bin is omitted since error velocities are generally too large, rendering the data unusable.

The temporal averaging described above applies an average over a window length of 2.5 h to the ADCP data. The influence of the time window's width on the accordance of the shipboard and satellite measured velocities is to be evaluated separately. Therefore, the averaging of the ship's data was repeated for time window lengths from 15 min to 24 h. For comparability all of these are averaged over depth within the reference layer.

A constant temporal sampling rate of the ADCP data does not mean that the spatial distance between two samples is constant. Since the ship's speed varies along the way, averaging the profiles into 2.5 h bins in fact produces distances between samples with an order of magnitude ranging from 100 m to 10 km. Therefore, a third scheme is tested in an attempt to match the spatial scale of the AVISO grid. After averaging all profiles within the reference layer, the resulting velocities are averaged into segments of fixed spatial width Δs along the track distance of the ship. Since the size of the AVISO grid is defined in terms of latitude and longitude the same is done for the ship's data. For a longitudinal displacement Δ_{lon} and a latitudinal displacement Δ_{lat} of the ship the distance Δs is set to be $\Delta s = \sqrt{\Delta_{\text{lon}}^2 + \Delta_{\text{lat}}^2} = 0.25°$.

The daily maps of AVISO velocities can be treated as a 3-dimensional grid with 2 spatial dimensions given as longitude and latitude and the 3$^{\text{rd}}$ dimension being time. To interpolate this grid to the ADCP's measurement times, an assumption has to be made in that each day's AVISO velocity must be assigned to a specific time of day. This time was chosen to be noon. Once the ADCP's data are averaged into a 1-dimensional time series in both velocity components, the interpolation of the AVISO velocities is done using a 2-dimensional linear interpolation within the spatial dimensions and a linear interpolation in time.

2.5. Tidal Correction

Ocean tides are to be removed from the ADCP data to achieve comparability with the absolute geostrophic AVISO velocities. It shall be assessed how large the effect of the tidal correction is in comparison to the signal magnitude and whether it reduces the difference between satellite and shipboard measurements.

Two different versions of the the *TPXO* model provided by the Oregon State University are used and compared. *TPXO* is an inverse model of satellite observational data. The model places two different types of constraints on it's tidal velocities: On the one hand they need to satisfy the Laplace Tidal Equations, on the other hand they need to best-fit, in a least-squares sense, direct observational satellite data from TOPEX/Poseidon and Jason. The way in which the model is computed from both data and dynamics is described by Egbert and A.F. Bennett (1994) and Egbert and Erofeeva (2002). The two model version of *TPXO* that are compared both to each other and to the uncorrected case are on the one hand *TPXO 7.2*, a global model on a 0.25° x 0.25° cartesian grid, and on the other hand the regional *TPXO 7.1 Atlantic Ocean* model which has a resolution of 1/12° x 1/12°.

2.6. Statistical Analysis of Co-Located ADCP and Altimeter Velocity Measurements

A consistent way of processing the ADCP data is applied to all 15 data sets. Of the different processing schemes that were tested on the MSM21/2 cruise the averaging over 2.5 h alongtrack and over depths from 46.5 m to 134.5 m will show to yield the best accordance with the satellite

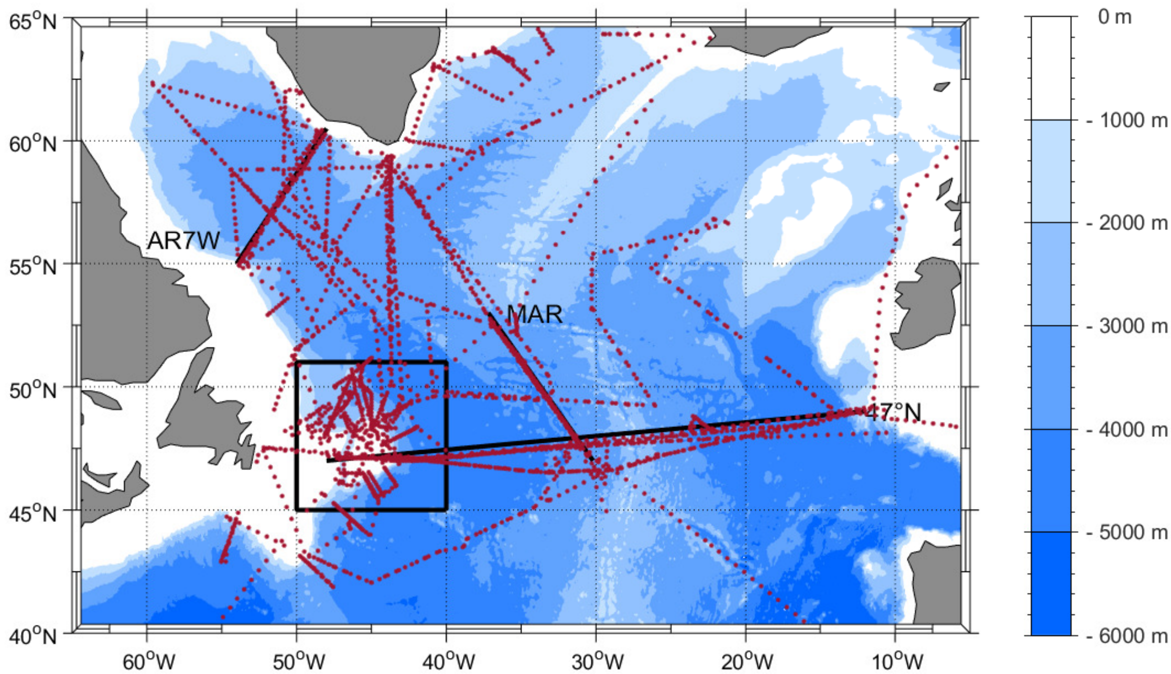

Figure 6: Ensemble of all velocity measurements obtained from averaging all 15 cruises' data sets. At each location indicated by a point in the map one measurement for both velocity components is given both from the ADCP and from the satellite data. The data clearly concentrates geographically along the 3 sections 47°N, AR7W and MAR marked by black lines as well as within a radius of roughly 300 km around Flemish Cap, marked by a black rectangle.

data and hence be used. This provides for an ensemble of 3346 averaged and tide-corrected shipboard measurements in both velocity components with their corresponding satellite measurements (Fig. 6). These measurements from two different instruments at identical times and positions are to be analysed with respect to their accordance. This includes quantifying the correlation as well as systematic and random deviations between the AVISO and the ADCP velocities. The linear relation between the satellite and the in-situ measurements is to be quantified by a linear regression and evaluated against the physical background.

The data along the 47°N section covered by multiple cruises will be be looked at separately. The ADCP measurements within one cruise present an accumulation of velocity snapshots at different positions and times. Repeated cruises along one section allow for the comparison of velocity measurements from different years at the same location. This comparison is made for the 47°N section stretching eastward from Flemish Cap. Both the shipboard measurements

Section	Cruises Covering Section
47°N	MSM5/1, MSM9/1, MSM12/3, MSM21/2, MSM27, MSM28, MSM38, MSM43, MSM53, MET59/2, MET85/1, ThalSP
AR7W	MSM12/3, MSM28, MSM43, MET85/1, ThalSP
MAR	MSM91, MSM212, MSM28, MSM38, MSM43, MSM53, MET85/1

Table 2: List of which section has been covered by which cruises. The sections may not necessarily have been covered to the full extent by each of the listed cruises.

of different cruises and the co-located AVISO velocities are interpolated to identical locations along the section. Hence there will be several independent measurements made in different years from both instruments at each new query point. It is then possible to compare both the variability and mean of these independent measurements along the 47°N section acquired by means of satellite altimetry and shipboard ADCP, respectively.

Furthermore, the spatial distribution of random deviations between satellite- and shipboard measurements is investigated. Therefore the ensemble is gridded in 2° x 2° boxes across the whole domain. Every pair of measurements of every cruise falling into one grid box contributes to the ensemble of that respective box. The rms deviation of all satellite and ADCP observations within one box gives a spatial representation of the random deviations. However, this will inevitably compare boxes with a large variety of measurements in each box, since the spatial concentration of measurements is very heterogeneous (Fig. 6).

2.7. Correlating ADCP Measured Transports and Satellite Measured Velocities

As before, ADCP data with a PG value below the threshold of 80 % is omitted. The depth profiles are then averaged along the cruise track using a time window length of 2.5 h. Subsequently the depth profiles are integrated in between 50 m and 550 m. This results in an ensemble of transport measurements that reflect the average volumetric transport per unit horizontal distance (m^2/s) within the domain that constitutes to the respective averaged measurement point. The depth range that is chosen here is the least prone to velocity errors. As has been mentioned before, the layers very close to the sea surface, i.e. around 0-50 m and close to the range of the ADCP, i.e. lower than roughly 600 m are characterized by large velocity errors. On

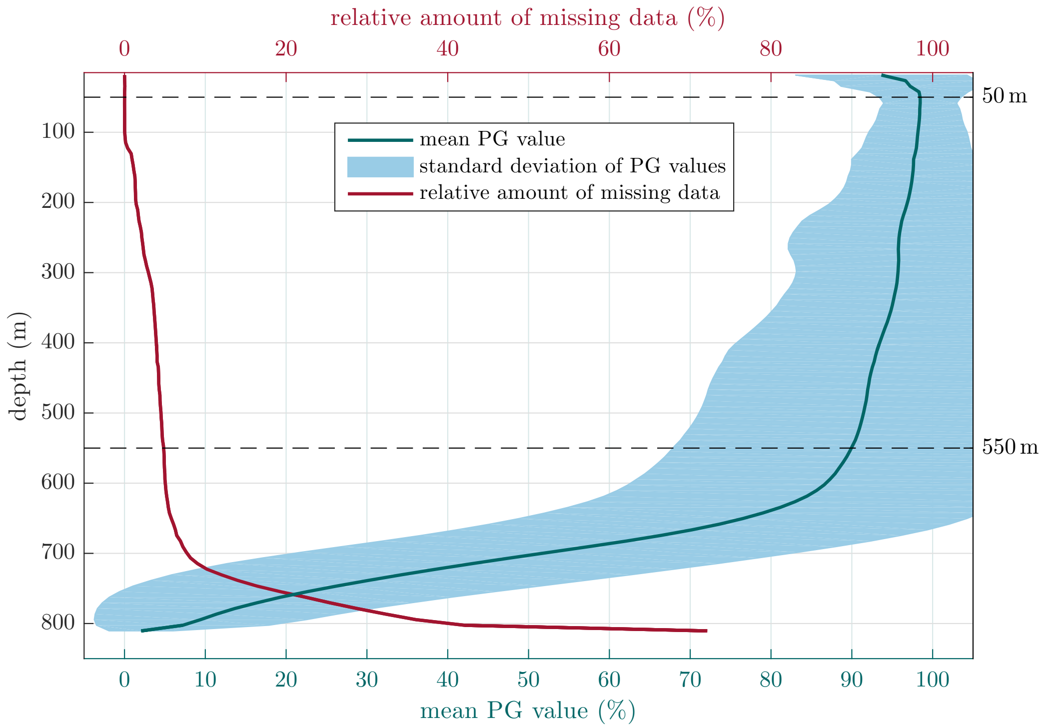

Figure 7: Average PG value and relative amount of missing data in the ADCP measurements of the MSM21/2 cruise. The mean PG value at a certain depth is the average of all PG values within that depth cell, the shaded area indicates the standard deviation of the PG values at the respective depth. The missing data is given as the percentage of all ADCP measurements taken on the MSM21/2 cruise.

the one hand this is indicated by the ADCP recording unreasonably high speeds (Fig. 4), on the other hand the mean PG value within one depth cell rapidly decreases below 550 m (Fig. 7). Furthermore the amount of missing velocity measurements increases with depth. For the case of the MSM21/2 cruise, there are less than 5% missing values above 600 m. Below this point the amount of valid velocity measurements strongly decreases.

Using all data sets listed in Tab. 1 except for the MSM27 data, which only reaches down to 410 m, a set of 3269 volumetric transport measurements is obtained that can be correlated with the AVISO velocity measurements. The linear relation between these, obtained through ordinary least squares regression (OLS), shall be used as a transfer function that enables the calculation of surface transport from satellite measured velocity. By taking 10000 bootstrap samples from the entire ensemble of measurements the transfer function's confidence intervals will be estimated.

Thereafter, this transfer function is to be applied to three sections which are traversed by several of the considered cruises. For each transect conducted by a cruise, the volumetric transports per horizontal distance across the section, as measured by the ADCP, are integrated along the section. The definite integral will be approximated with the trapezoidal rule. Calculating the transport from the satellite's velocity observations requires an interpolation of the gridded data onto the respective section, which is parametrized as a straight line. Since a research vessel does usually not pass the sections of interest within one day, the satellite data is averaged over the respective time it took the ship to cover the section. Using the transfer function the velocities are subsequently converted into transports and integrated along the section, using again the trapezoidal rule.

The first of the three sections is the 47°N section in between 46.875°W and 31.375°W. 6 of the 12 cruises that passed this section took a very similar route that allows for the use of one parametrisation for all 6 cruises (MSM12/3, MSM21/2, MSM28, MSM38, MSM43, MET85/1). Therefore only these 6 are considered. The second section is west of the Mid Atlantic Ridge and labelled MAR in the following. It reaches from 36.031°W/51.875°N in the north-west to 31.614°W/48.125°N in the south-east. The MAR section has been covered by 7 of the cruises that were analysed (MSM9/1, MSM21/2, MSM28, MSM38, MSM43, MSM53, MET85/1). All 7 of these partly passed the section twice – the data was therefore divided into 2 parts, since the transport across the section varies significantly in between days. The third section that was looked at is the AR7W located in between 48.375°W/60.191°N in the north-east and 53.677°W/55.125°N in the south-west, i.e. spanning the Labrador Sea from the southern tip of Greenland to Hamilton Bank. It was covered by 5 cruises (MSM12/3, MSM28, MSM43, MET85/1, ThalSP), though only by 3 of these to its full extent.

Furthermore, the AVISO satellite data available for the time from January 1993 to May 2016 will be used to calculate a 24-year timeseries of volumetric surface transports across each of these three sections. These timeseries are to be evaluated taking into account the way the velocities were transferred to transports as well as the resulting uncertainty in the transport values.

3. Results

The results' description is structured into three parts as follows: First of all the different averaging schemes and tidal corrections applied to the ADCP data of the MSM21/2 cruise will be assessed and compared. Thereafter, the statistical analysis of the ensemble of all cruises' ADCP data is given. The last part is concerned with the calculation of surface transports, correlating the ADCP transports to AVISO velocities on the one hand and looking at specific transports across the 47°N, AR7W and MAR section on the other hand.

3.1. Processing the MSM21/2 ADCP Data

Three averaging schemes described in section 2 yield one time series per scheme and velocity component. In each case the AVISO data has been interpolated to a time series at identical positions and times for each velocity component u, v. Three parameters shall characterize the accordance of these. The first diagnostic quantity is the root-mean-square of the time series' difference

$$\mathrm{rms}(u_{\mathrm{ship}}, u_{\mathrm{satellite}}) = \sqrt{\frac{1}{N}\sum_{i=1}^{N}(u_{\mathrm{ship},i} - u_{\mathrm{satellite},i})^2} \tag{13}$$

in which $u_{\mathrm{ship},i}$ and $u_{\mathrm{satellite},i}$ are the ships and the satellites velocity measurements at location $\vec{x}_i$ and time t_i. The rms quantifies the absolute difference between individual measurement points. In the following these rms differences are abbreviated as root-mean-square deviation (rmsd), where rmsd_u and rmsd_v will refer to the zonal and meridional component, respectively. Secondly, the bias is calculated as the mean of all deviations

$$\mathrm{bias}(u_{\mathrm{ship}}, u_{\mathrm{satellite}}) = \frac{1}{N}\sum_{i=1}^{N}(u_{\mathrm{ship},i} - u_{\mathrm{satellite},i}) \tag{14}$$

and thereby estimates in how far positive and negative offsets between the time series cancel each other out over the whole cruise. It is used to measure whether one of the instruments systematically records larger values than the other. $\mathrm{bias}(u/v_{\mathrm{ship}}, u/v_{\mathrm{satellite}})$ are hereafter referred to as $\mathrm{bias}_{u/v}$. As a third parameter the linear correlation coefficient of the ship's and the satellite's measurements quantifies their linear dependence on each other. Below, it is denoted corr_u and corr_v, respectively.

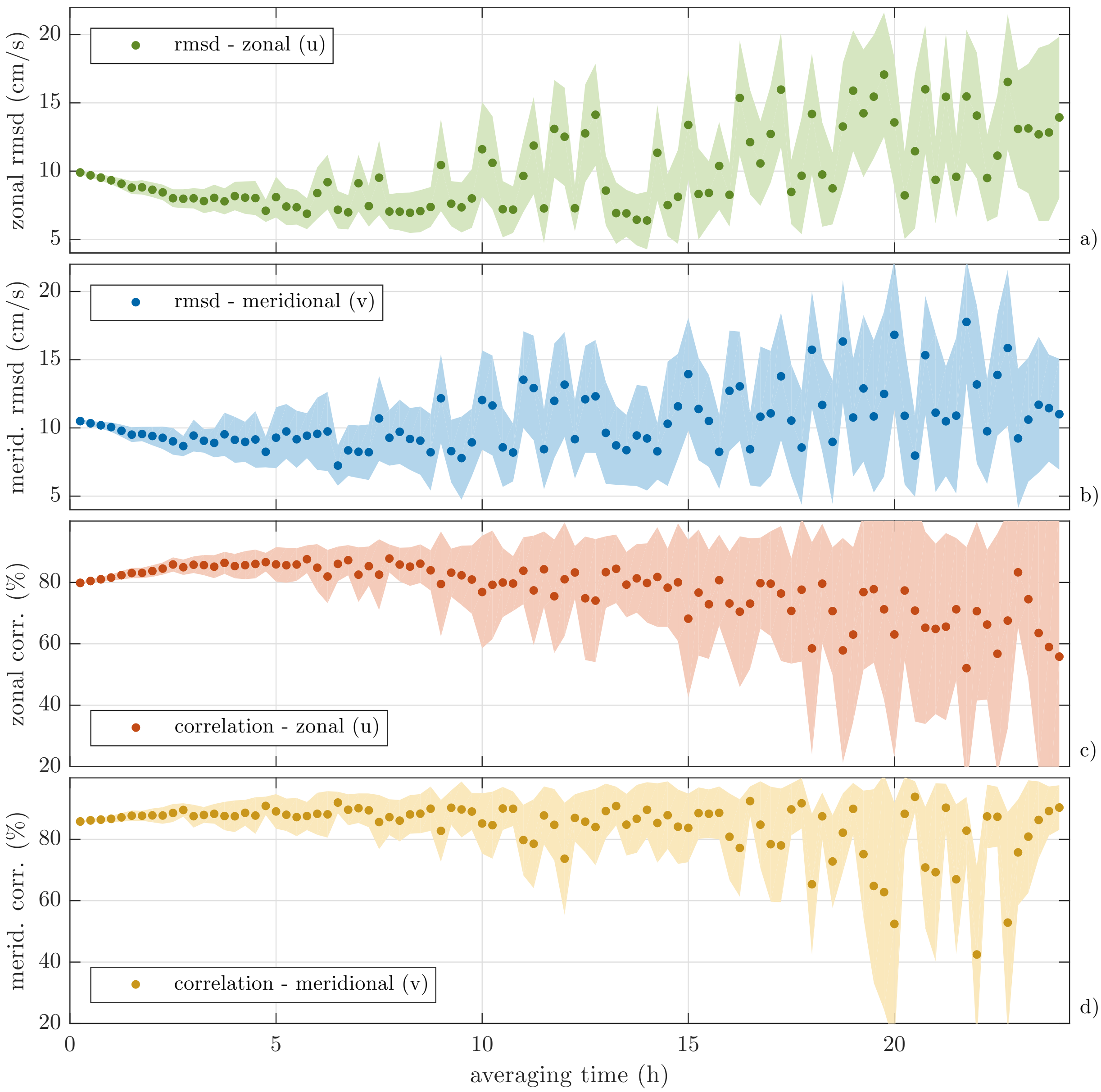

Figure 8: Dependence of the accordance between satellite- and ADCP measured velocities on averaging time: rmsd (panel a) and b)) and correlation (panel c) and d)) of the time series for averaging times from 15 min to 24 h. All values are obtained by taking the ADCP profiles' mean value over depth from 46.5 m to 134.5 m. The tinted area displays the parameters' uncertainty estimates propagated from the shipboard ADCP's standard deviation.

3.1.1 Comparison of Averaging Times

The time over which the ADCP's data are averaged along the cruise track largely influences the accordance with the satellite's data (Fig. 8). Averaging over the reference layer, the time window length is varied from 15 min to 24 h. For 15 min averages $\text{rmsd}_u = (9.9 \pm 0.2)\,\text{cm}\,\text{s}^{-1}$ and $\text{rmsd}_v = (10.5 \pm 0.2)\,\text{cm}\,\text{s}^{-1}$; these values decrease in both velocity components with increasing averaging time up to about 2.5 h. Beyond this point the rmsd increases overall, though not following a monotonic trend. The correlation shows a similar behaviour, increasing up to $\text{corr}_u = (85.9 \pm 2.4)\,\%$ and $\text{corr}_v = (88.6 \pm 3.0)\,\%$ at an averaging time of 2.5 h. Both corr_u and corr_v stay above 80 % for averaging times of 5 h to 10 h and decrease for longer times, though not monotonically.

It has to be mentioned that for large averaging times, the uncertainties displayed in Fig. 8 present a poor estimate for the uncertainty of the rmsd/correlation values. Since these intervals are propagated from the standard deviation of all velocity measurements contributing to one mean velocity, they rather reflect on the large variance of velocities within the averaging interval than on the precision of the rmsd/correlation estimate, as shall be elaborated in the discussion.

3.1.2 Evaluation of Tidal Correction

Both the global model *TPXO 7.2* and the regional model *TPXO 7.1 Alantic Ocean* predict tidal velocities that range from $-6.1\,\text{cm}\,\text{s}^{-1}$ to $5.6\,\text{cm}\,\text{s}^{-1}$ in zonal direction and respectively from $-7.9\,\text{cm}\,\text{s}^{-1}$ to $6.5\,\text{cm}\,\text{s}^{-1}$ in meridional direction for the MSM21/2 cruise. These predictions have a standard deviation of $2.1\,\text{cm}\,\text{s}^{-1}$ in the zonal and $1.4\,\text{cm}\,\text{s}^{-1}$ in the meridional component. Both models largely predict identical velocities except at the Flemish Cap at 47.1°N in the time from 6 July to 9 July (Fig. 9). This can be attributed to the fact that tidal velocities are generally smaller in the open ocean than they are in shallow waters; the Flemish Cap is the only part of the MSM21/2 cruise where the ocean is shallower than 1000m (Fig. 5).

The accordance between the ADCP's and the satellite's signal does not depend strongly on the tidal correction over the whole cruise: Using an averaging over the reference layer and a 2.5 h average, the rmsd is reduced by as little as $0.3\,\text{cm}\,\text{s}^{-1}$ to $(8.0 \pm 0.7)\,\text{cm}\,\text{s}^{-1}$ in the u component and by $0.03\,\text{cm}\,\text{s}^{-1}$ to $(9.02 \pm 1.00)\,\text{cm}\,\text{s}^{-1}$ in the v component. These rmsd values are identical for both the *TPXO 7.2* and the *TPXO 7.1 Alantic Ocean* tidal model. Equally the bias does only change in the order of $0.01\,\text{cm}\,\text{s}^{-1}$ and the correlation in the order of 0.1 % in both velocity components (Fig. 10). Notably the changes do not exceed the values' uncertainty estimates.

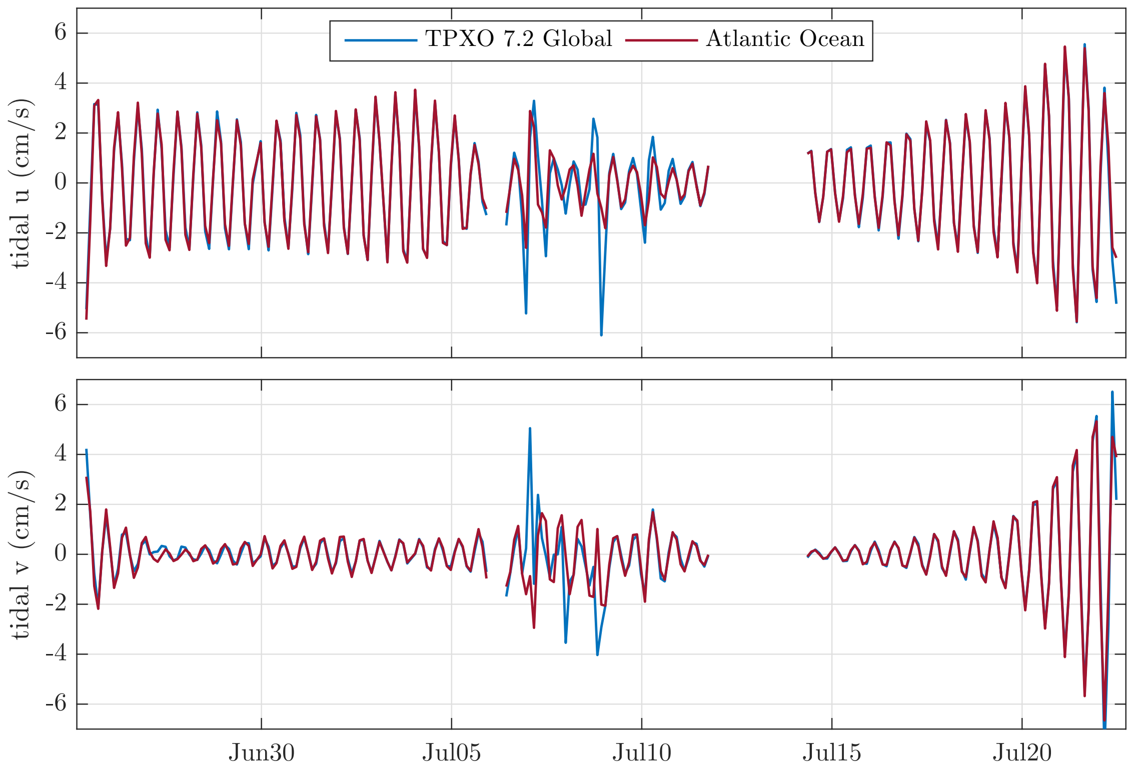

Figure 9: Prediction of tidal velocities in zonal (u, upper panel) and meridional (v, lower panel) direction; both the global model with coarse resolution (*TPXO 7.2 Global*) and the finer regional model (*Atlantic Ocean*) are fed with the locations and times of the averaged time series, using a 2.5 h averaging window; missing parts in the prediction correspond to days without ADCP measurements.

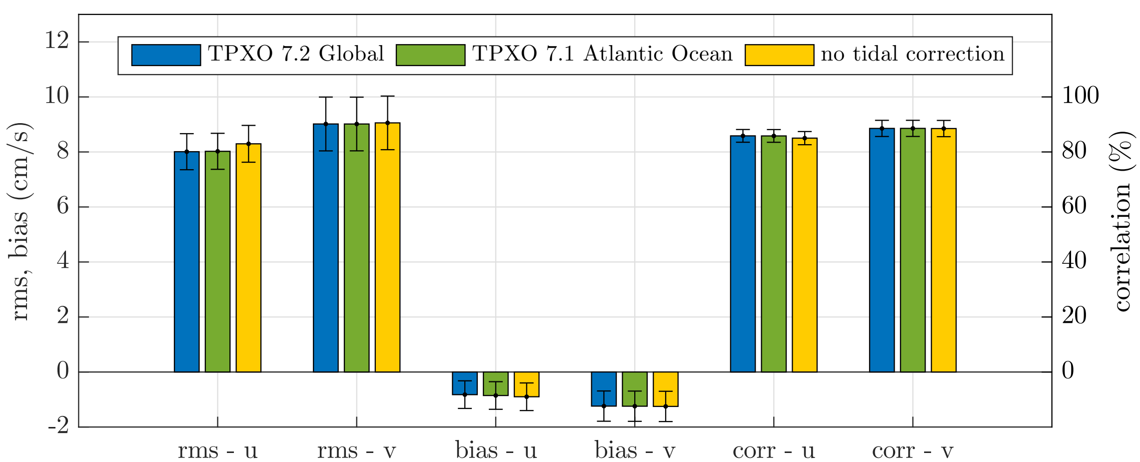

Figure 10: Comparison of deviations between satellite- and ADCP measured velocities with and without tidal correction of the shipboard measured data. The rmsd and bias of the deviations are shown next to the correlation of the time series for both tidal models and the uncorrected velocities. A negative bias corresponds to satellite velocities being larger than ship velocities.

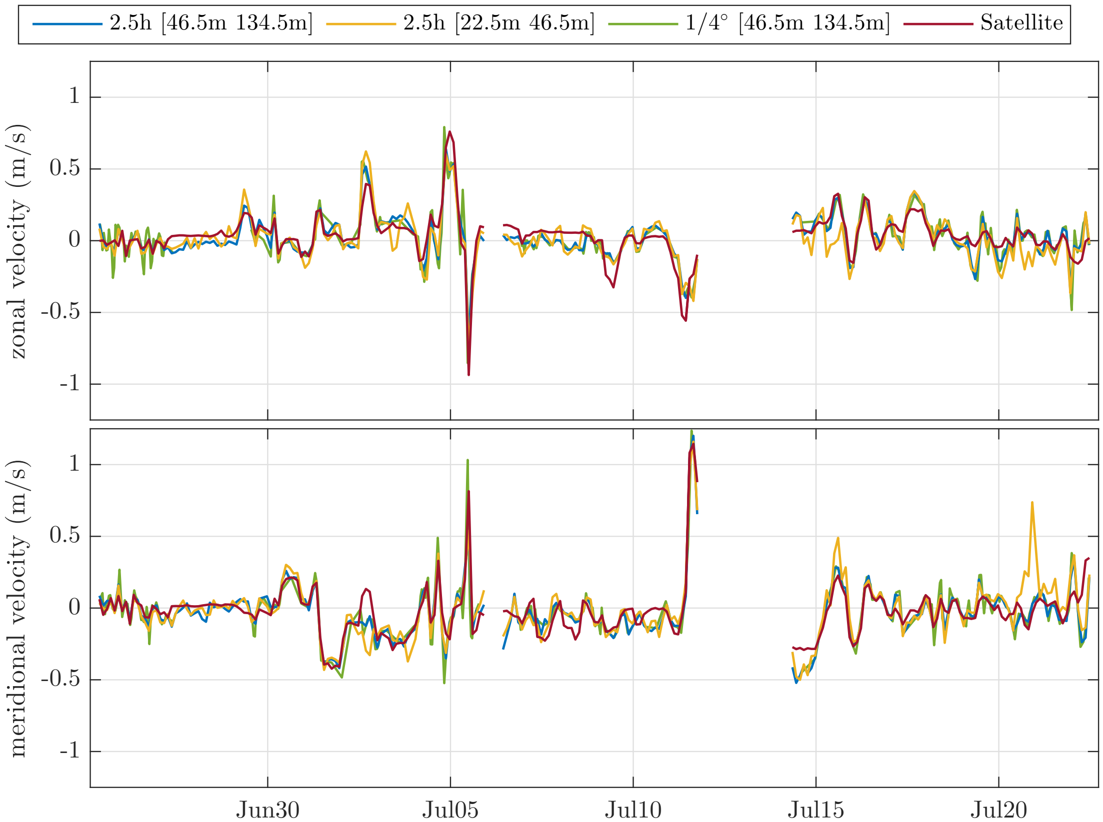

Figure 11: Comparison of satellite- and ADCP measured velocities in zonal (upper panel) and meridional (lower panel) direction; in both panels three different ADCP velocities are shown which correspond to three different averaging schemes as denoted in the legend; all three include a tidal correction using the *TPXO 7.2* global model.

3.1.3 Comparison of Averaging Schemes

All time series obtained by the three different averaging schemes display the same general features as the one that is interpolated from the satellite altimetric measurements (Fig. 11). Notably in the case of large velocities, that is in the order of magnitude of $10\,\mathrm{cm\,s^{-1}}$ all four curves show a similar behaviour. The choice of the depth range that is considered has a stronger effect on the result than the choice between spatial or temporal averaging. The two schemes considering the reference layer coincide to a large extent, while considering the surface layer yields large deviations from these.

The rmsd, bias and correlation between ADCP and satellite measurements differ for all three averaging schemes (Fig. 12). They indicate the best accordance for the case of a

2.5 h average over depths within the reference layer (from 46.5 m to 134.5 m). In that case $\text{rmsd}_u = (8.0 \pm 0.7)\,\text{cm}\,\text{s}^{-1}$ and $\text{rmsd}_v = (9.0 \pm 1.0)\,\text{cm}\,\text{s}^{-1}$ as opposed to values of $\text{rmsd}_u = (10.0 \pm 1.2)\,\text{cm}\,\text{s}^{-1}$ and $\text{rmsd}_v = (10.7 \pm 1.4)\,\text{cm}\,\text{s}^{-1}$ for a temporal averaging in the surface layer (from 22.5 m to 46.5 m). A spatial averaging in the reference layer yields $\text{rmsd}_u = (10.2 \pm 0.5)\,\text{cm}\,\text{s}^{-1}$ and $\text{rmsd}_v = (10.6 \pm 0.6)\,\text{cm}\,\text{s}^{-1}$. Similarly with $\text{corr}_u = (85.9 \pm 2.3)\,\%$ and respectively $\text{corr}_v = (88.6 \pm 3.0)\,\%$ the correlation is highest for a temporal averaging in the reference layer, while it is smallest for a temporal averaging in the surface layer in both velocity components. The bias does not show such a coherent behaviour, it's magnitude is not smallest in both velocity components for any of the three compared cases.

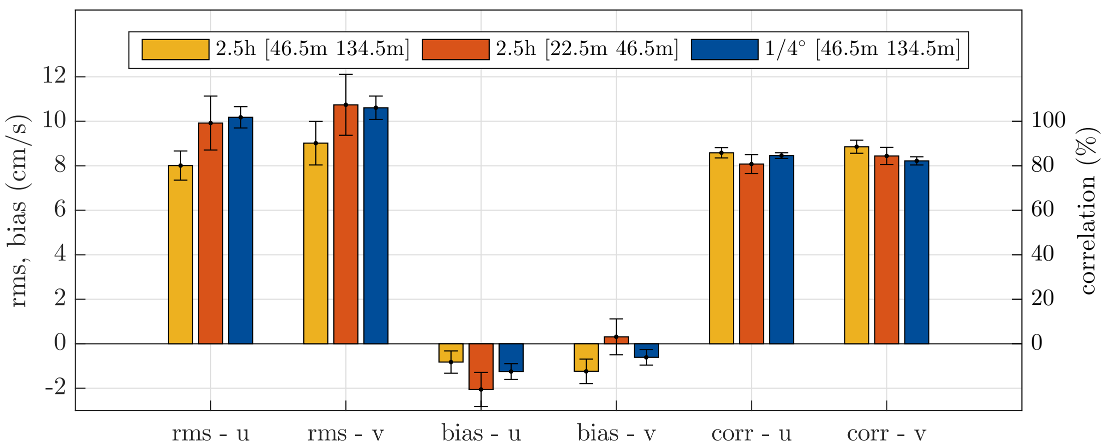

Figure 12: Comparison of deviations between satellite- and ADCP measured velocities, averaged with three different schemes as denoted in the legend; all three include a tidal correction using the *TPXO 7.2* global model; for all three averaging schemes the rmsd and bias of the deviations are shown next to the correlation of the time series.

3.2. Statistical Analysis of Co-Located ADCP and Altimeter Velocity Measurements

An ensemble of 15 cruises' ADCP data, averaged into bins of 2.5 h as described above, provides for an overall of 3346 velocity measurements in both velocity components u and v. As was the case before, the overall accordance of these with their respective satellite measurements is to be quantified by the root-mean-squared difference ($\text{rmsd}_{u/v}$), the mean difference ($\text{bias}_{u/v}$) and the correlation ($\text{corr}_{u/v}$) between the two time series. After assessing these diagnostic parameters, the linear relationship between satellite measurements and shipboard measurements is to be looked at in detail. A common pattern of discordance is discussed which describes the deviation

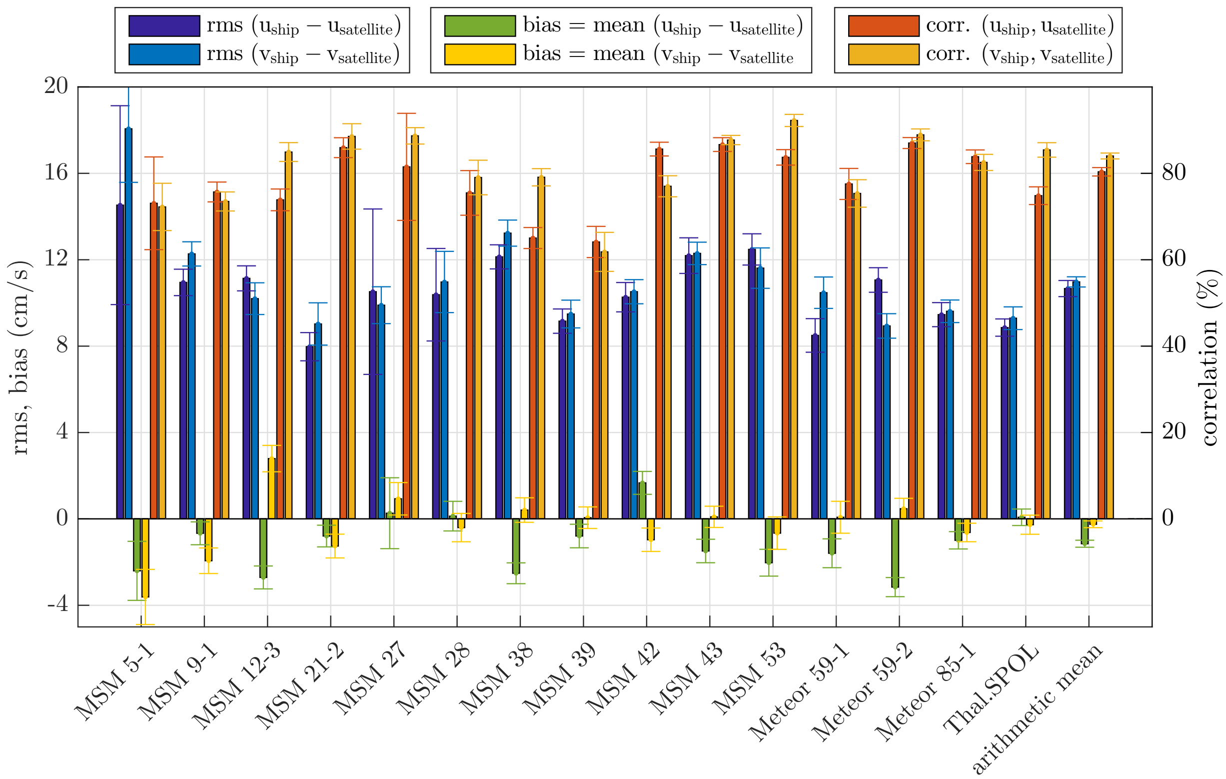

Figure 13: Comparison of deviations between satellite- and ADCP measured velocities for 15 cruises, denoted along the abscissa, as well as for the ensemble of all cruises' measurements. For each individual cruise the rmsd and bias of the deviations are shown next to the correlation of the time series as indicated by the legend. A negative bias corresponds to satellite velocities being larger than ship velocities. The uncertainties of the depicted diagnostic parameters are estimated based on the standard deviation of the ADCP measurements – that is, the variance of the velocities within the section along the cruise track that contributes to one averaged ADCP measurement is taken to be an estimator for it's variance.

of altimetric and in-situ observations qualitatively. Moreover, the spatial distribution of rms deviations between the two instruments' time series is evaluated. Finally the measurements along the 47° section are regarded separately.

3.2.1 Analysis of Multiple Cruises' Velocity Data

The rmsd values scatter lightly around an all-cruise mean which is nearly identical for the zonal and meridional component, being $(10.7 \pm 0.4)\,\mathrm{cm\,s^{-1}}$ and $(11.0 \pm 0.3)\,\mathrm{cm\,s^{-1}}$ respectively (Fig. 13). Compared to an averaged absolute signal of $12.9\,\mathrm{cm\,s^{-1}}$ these deviations are relatively high and suggest little accordance at first sight. In contrast the correlation ranges between $(61.8 \pm 4.6)\,\%$ and $(92.2 \pm 1.5)\,\%$ for all 15 cruises, where the average correlation is slightly

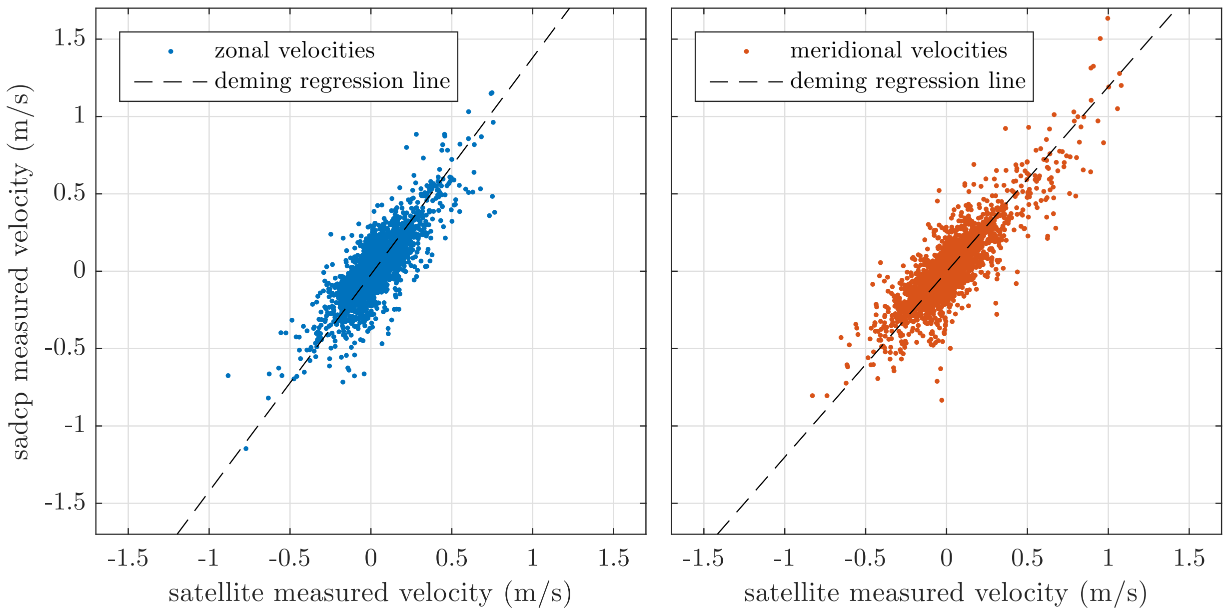

Figure 14: 3346 ADCP measurments taken along 15 cruises are plotted against the AVISO satellite measurements made at the same respective time and location. The regression line describes the linear relation to be $u_{\text{ship}} = 1.40 \cdot u_{\text{sattelite}} - 2.1\,\text{cm}\,\text{s}^{-1}$ for the zonal and $v_{\text{ship}} = 1.20 \cdot v_{\text{sattelite}} - 0.4\,\text{cm}\,\text{s}^{-1}$ for the meridional component, respectively. The deming regression used here minimizes the sum of the measurements' orthogonal distance to the line of best fit, in contrast to an ordinary linear regression minimizing the distance solely along the ordinate (Xu, 2014).

higher in the meridional component with a value of (84.0 ± 1.0) %, compared to (80.4 ± 0.7) % in the zonal component. The discrepancy between high correlation on the one hand and high rmsd on the other hand can easily be understood by plotting the ADCP measurements against those of the satellite and performing an orthogonal linear regression (Fig. 14). While the data are tightly scattered about the regression line in both velocity components, reflecting the high correlation, this line has a slope significantly larger than unity in both velocity components, being 1.40 in the zonal and 1.20 in the meridional component and causing the absolute deviations to be high despite the linear dependence. The bias between both time series is an order of magnitude smaller than the rmsd, varying from $(-3.6 \pm 1.3)\,\text{cm}\,\text{s}^{-1}$ to $(2.8 \pm 0.7)\,\text{cm}\,\text{s}^{-1}$ with a mean of $(-1.1 \pm 0.2)\,\text{cm}\,\text{s}^{-1}$ and $(-0.2 \pm 0.2)\,\text{cm}\,\text{s}^{-1}$ in the meridional and zonal component, respectively. So the mean systematic deviation is not only relatively small compared to the mean absolute signal, but also negative, i.e. the satellite measured signal is larger than that measured by means of ADCP. The linear relation however quantifies how the satellite generally underestimates the signal as measured by the ADCP – not in the sense that the satellite's mean signal is lower than the SADCP's, but rather in that its magnitude is smaller. This behaviour can be illustrated by a pattern of discordance which occurs repeatedly for different cruises' data. Suppose that the ADCP measures fluctuations around 0 velocity, i.e. the recorded velocity changes its direction. While the satellite measurements may follow this flow, recording the change in direction, they often lack to reproduce the ship's measurements in recording lower magnitudes. The altimetric velocities appear to be dampened compared to the ADCP observations, figuratively they do not *fill* the ADCP's peaks (Fig. 15).

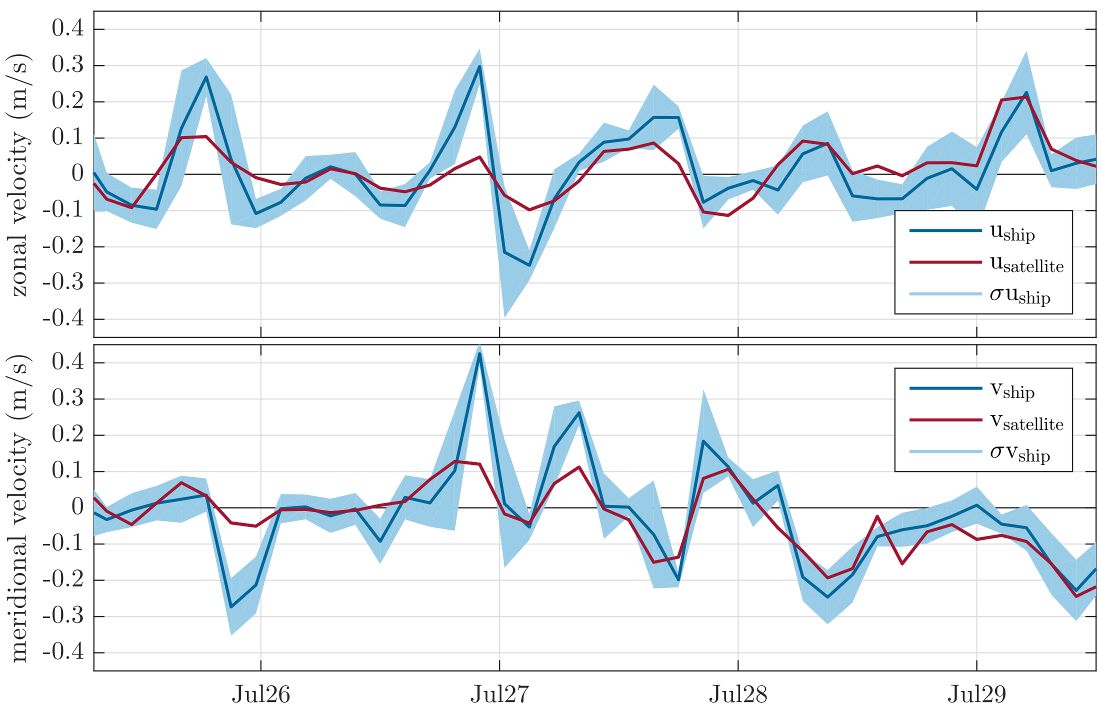

Figure 15: Example for a typical pattern of discordance between the surface velocity measured by shipboard ADCP and that measured by satellite altimetry. The ADCP measurements where conducted during the MSM12/3 cruise in 2009. The shaded area represents the standard deviation of the ADCP velocities. While both instruments record the flow to be in the same direction, they disagree in the recorded speed. This is particularly pronounced for the time from July 25 to July 27, where the magnitude of the satellite's signal stays clearly below the uncertainty range of the ADCP's signal.

3.2.2 Spatial Distribution of Deviations

The rmsd, bias and correlation values calculated over either whole cruises or the ensemble of all 15 cruises cannot account for the spatial variation in the contributing measurements.

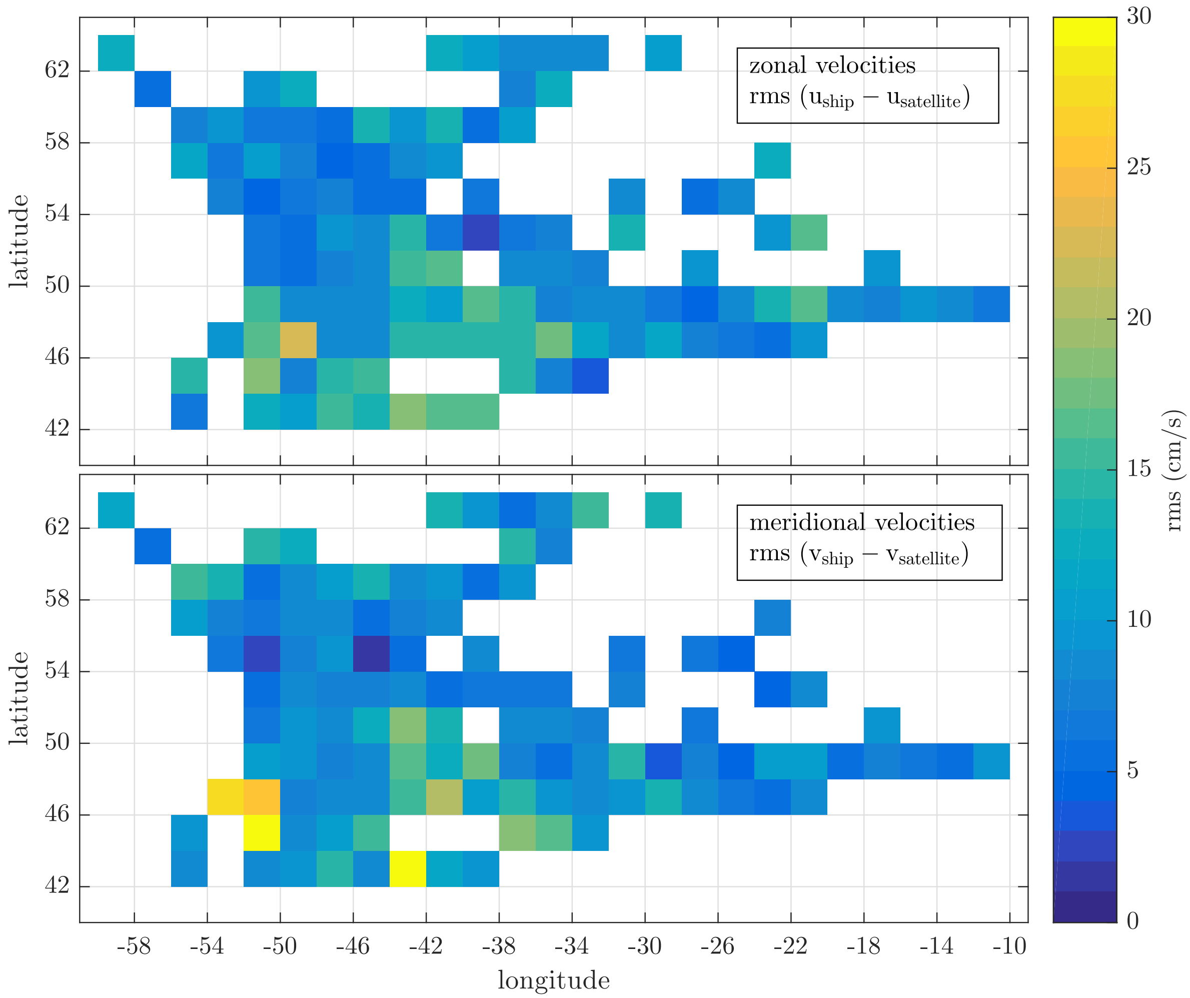

Figure 16: Spatial distribution of deviations of shipboard velocity measurements from those measured by satellite altimetry. Both panels show the ensemble of measurements taken along 15 different cruises in the subpolar North Atlantic. In every grid box the root-mean-square deviation of all shipboard- and satellite measurements falling into that respective box is shown. Grid cells with less than 5 measurement pairs have been neglected. The upper limit of the colorscale includes all rmsd values larger than 30 m/s.

In an attempt to quantify the spatial variability of rms deviations, these are evaluated on a 2° x 2° grid, where every pair of measurements of every cruise falling into one grid box contributes to its rmsd (Fig. 16). Their distribution indicates that in both velocity components the deviations that are higher than the average of 11 $\mathrm{cm\,s^{-1}}$ concentrate mainly in two areas, where the first can be described as a patch centred around 40°W/47°N stretching over roughly 10° in both longitudinal and latitudinal direction; the second area is located on the grand banks, where particularly in the meridional velocities both instruments disagree strongly. The graphical evaluation shows no finer spatial structure of the discordances than the described coarse arrangement. Notably these deviations show no systematic variation with the number of measurements contributing to one value. This number of ADCP measurements found in one grid box varies largerly from 1 to 285 values. Cells with less than 5 values make up ca. 36 % of all cells. Having neglected these in the analysis, roughly 37 % of the remaining boxes contain 5 to 9 values.

3.2.3 Evaluation along the 47°N Section

Within one cruise the shipboard ADCP measurements present an accumulation of velocity snapshots at different positions and times. Comparing the results obtained during different cruises inevitably compares measurements of different times taken at partly different regions. Repeated cruises along the transatlantic section from 47°W to 17°W at 47°N allow for the comparison of velocity measurements at the same location. 12 cruises along this section, conducted in 11 different years in between 2003 and 2016 have been averaged to evaluate whether the accordance between satellite and ADCP measurements will rise in the case of averaging of repeated measurements.

In the following 2 different rmsd values will be compared: On the one hand there is one rmsd value for each individual cruise's velocity observation and the corresponding AVISO velocities. The average over all 12 of these will be referred to as *cruises' mean* rmsd. On the other hand there is the rmsd of the averaged velocities of 12 cruises and the average of the co-located satellite measurements which is referred to as rmsd of the averaged velocities. The same goes for the correlation parameter as well as for the maximal velocities that where observed during each of the 12 individual cruises compared to that of the averaged velocity field.

While the rmsd along the complete section is relatively high for the individual cruises with a cruises' mean rmsd of $(12.6 \pm 0.5)\,\mathrm{cm\,s^{-1}}$ in both velocity components, the averaged velocities agree to a greater extent with an rmsd of $(5.0 \pm 0.7)\,\mathrm{cm\,s^{-1}}$ and $(4.4 \pm 0.8)\,\mathrm{cm\,s^{-1}}$ in the u and v component, respectively. The repeated section along 47°N passes the North Atlantic Circulation (NAC) as well as it's recirculation. These undergo large temporal variability in their magnitude and position. Over the 12 measurements that are considered here, the maximum meridional velocity ranges from $(49.4 \pm 8.9)\,\mathrm{cm\,s^{-1}}$ to $(163.4 \pm 14.3)\,\mathrm{cm\,s^{-1}}$ around a cruises' mean of $90.7\,\mathrm{cm\,s^{-1}}$. During the 12 cruises whose observations are being evaluated, the maximum northward velocity was located in between 42.8°W and 40.2°W around a cruises' mean position of 41.1°W. Despite the large longitudinal shift of the NAC over the different measurement years both the northward flow and the recirculation are still pronounced in the average velocity field (Fig. 17), with the maximal magnitudes of $(47.7 \pm 12.3)\,\mathrm{cm\,s^{-1}}$ and $(-25.5 \pm 5.1)\,\mathrm{cm\,s^{-1}}$ being located at 40.3°W and 38.3°W, respectively. As was the case before, individual cruises' ADCP measurements show large correlation with the respective satellite measurements despite their large rmsd. The cruises' mean correlation is $(77.1 \pm 2.1)\,\%$ in the zonal and $(87.7 \pm 0.9)\,\%$ in the meridional component, respectively. The correlation is still slightly higher for the case of the averaged section with $\mathrm{corr}_u = (81.8 \pm 5.0)\,\%$ and $\mathrm{corr}_v = (93.2 \pm 2.3)\,\%$.

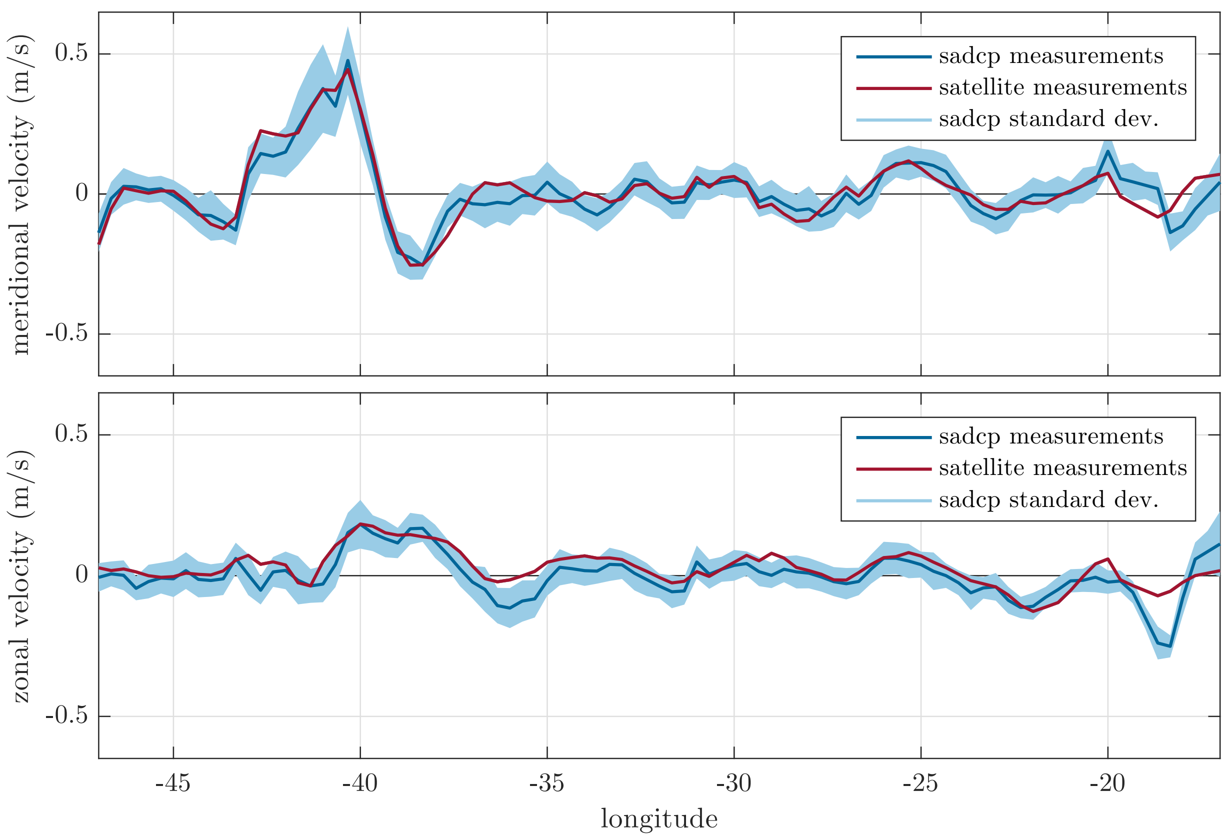

Figure 17: Comparison of averaged ADCP and satellite measurements along the section at 47°N. The velocity measurements conducted during 12 cruises were interpolated to evenly spaced longitudes and then averaged at each respective longitude. Not all of the 12 cruises covered the section to the full extent, hence the number of cruises contributing to the shown mean velocities differs with longitude.

3.3. Transferring Satellite Velocities to Surface Transports

The velocity depth profiles measured by the shipboard ADCP allow for the calculation of volumetric transports within the range of the instrument. For 14 of the cruises listed above, the profiles have been integrated in between 50 m and 550 m to obtain the volumetric transport per 1 m of horizontal distance normal to its direction. In the following these 3269 surface transport values taken in between June 2003 and May 2016, scattered across the subpolar North Atlantic, are to be related to the satellite altimetric velocity measurements taken at the same time and location respectively. Taking the AVISO velocities as a predictor of the surface transports, an ordinary linear regression (OLS) is used in both velocity components separately to calculate a transfer function that links surface velocity and upper-layer transport. Thereafter, this function is tested on the 47°N , MAR- and AR7W section, comparing the direct shipboard transport measurements to those obtained via the transfer function. Moreover, the transfer function is applied to the available 23 years of satellite velocity data, calculating a timeseries of transport across each respective section.

3.3.1 The Transfer Function

The surface transports measured by the ADCP exhibit a strong correlation with the geostrophic surface velocities measured by the AVISO satellite, which is $(81.0 \pm 1.4)\,\%$ in the zonal and $(82.4 \pm 1.0)\,\%$ in the meridional component (Fig. 18). An OLS using the satellite velocities u_{sat} and v_{sat} as a predictor for the ADCP measured transport U_{ACDP} and V_{ACDP} gives a linear relation for each velocity component:

$$U_{\mathrm{ACDP}} = m_{\mathrm{u}} \cdot u_{\mathrm{sat}} + c_{\mathrm{u}} = 451.5\,\mathrm{m} \cdot u_{\mathrm{sat}} - 7.0\,\mathrm{m}^2/\mathrm{s} \tag{15}$$

$$V_{\mathrm{ACDP}} = m_{\mathrm{v}} \cdot v_{\mathrm{sat}} + c_{\mathrm{v}} = 417.5\,\mathrm{m} \cdot v_{\mathrm{sat}} - 3.8\,\mathrm{m}^2/\mathrm{s} \tag{16}$$

The two times two parameters of the slope $m_{\mathrm{u,v}}$ and intercept $c_{\mathrm{u,v}}$ of two velocity components estimated here are based solely on the correlation of the two large datasets as opposed to the agreement of individual measurement pairs, which is not possible since two related but nonetheless different physical quantities are being compared. In order to estimate a confidence interval, standard error and bias as measures of accuracy for these, 10000 Bootstrap samples are taken from the empirical distribution of 2-dimensional satellite velocities and ADCP transports (Fig. 19). The slope and intercept calculated from the i-th bootstrap sample $(u_{\mathrm{sat},i}{}^{*}, v^{*}_{\mathrm{sat},i}, U^{*}_{\mathrm{ACDP},i}, V^{*}_{\mathrm{ACDP},i})$ will be denoted as $(m^{*}_{\mathrm{u},i}, m^{*}_{\mathrm{v},i}, c^{*}_{\mathrm{u},i}, c^{*}_{\mathrm{v},i})$, while the mean values

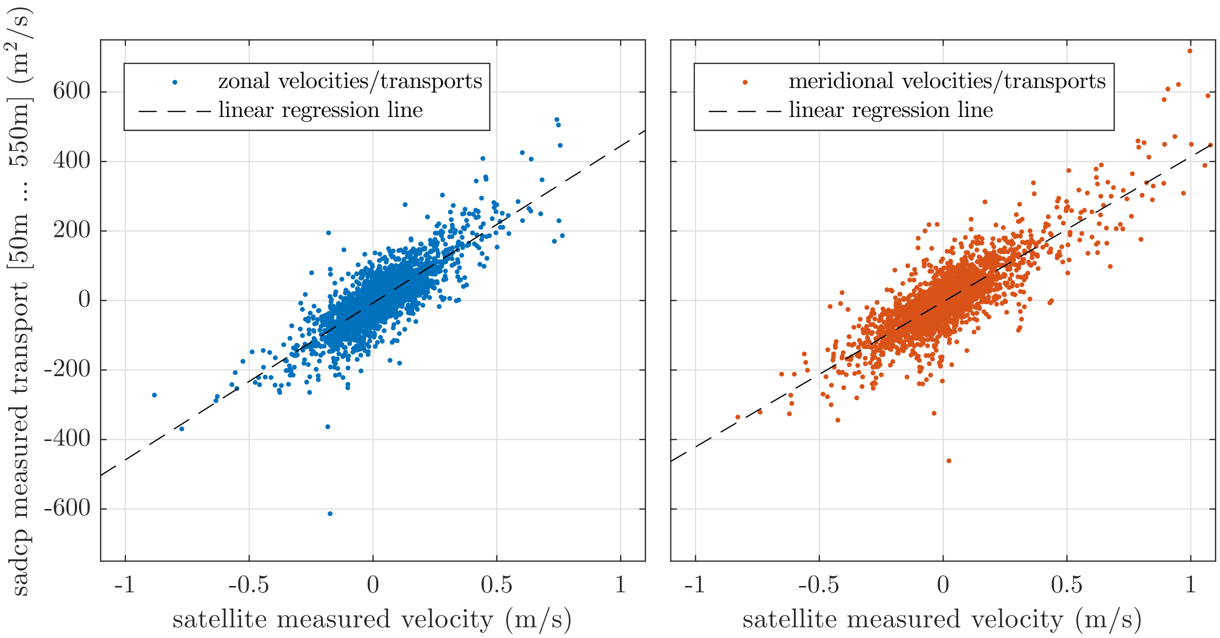

Figure 18: An ensemble of 3269 individual shipboard ADCP transport measurements in the upper ocean layer from 50 m to 550 m are plotted against the AVISO surface velocity measurements taken at the same time and location. Both for the zonal velocities shown in the left panel and the meridional velocities shown in the right panel the data is depicted alongside the dashed OLS regression line.

of the bootstrap estimates are denoted as $(\overline{m^*_\mathrm{u}}, \overline{m^*_\mathrm{v}}, \overline{c^*_\mathrm{u}}, \overline{c^*_\mathrm{v}})$. For each one of the four parameters, a standard error σ_x of parameter x can then be estimated from the bootstrap distribution to be

$$\sigma_x = \sqrt{\frac{1}{B-1}\sum_{i=1}\left(x^*_i - \overline{x^*}\right)^2} \tag{17}$$

where B is the number of bootstrap samples x^*_i (e.g. Wehrens et al., 2000). Furthermore, the bootstrap distribution is used to obtain a confidence interval of the transfer parameters. The empiric parameters are summarized alongside their corresponding bootstrap mean value, standard error and 95 % confidence interval in Tab. 3. The bias of parameter x can be similarly estimated from the distribution of it's bootstrap samples to be $bias_x = \overline{x^*} - \overline{x}$. However, it is small enough for all 4 parameters to be considered negligible, being below 0.4 % of the respective parameter.

The linear relation underlying the transfer function set up here seems to break down for large transports exceeding 400 m^{2}s^{-1}. The largest transport measurements, found mainly in the meridional component, are not centred about the regression line but clearly biased above it.

Parameter	Empirical Estimate	Standard Error	95 % Confidence Int.	relative bias
m_u	451.5 m	8.8 m	[434.4, 468.8] m	0.00 %
c_u	$-7.0\,m^2/s$	$0.8\,m^2/s$	$[-8.5,\ -5.4]\,m^2/s$	0.01 %
m_v	417.5 m	8.2 m	[401.4, 433.3] m	0.04 %
c_v	$-3.8\,m^2/s$	$0.9\,m^2/s$	$[-5.5,\ -2.1]\,m^2/s$	0.40 %

Table 3: Summary of the intercept and slope paramters (m_u, c_u, m_v, v_v used to described the linear relation between satellite velocities and surface transports. The empirical estimate is based on the OLS of the underlying data while the standard error as well as the confidence interval are calculated from the distribution of 10000 bootstrap samples of the 4 parameters.

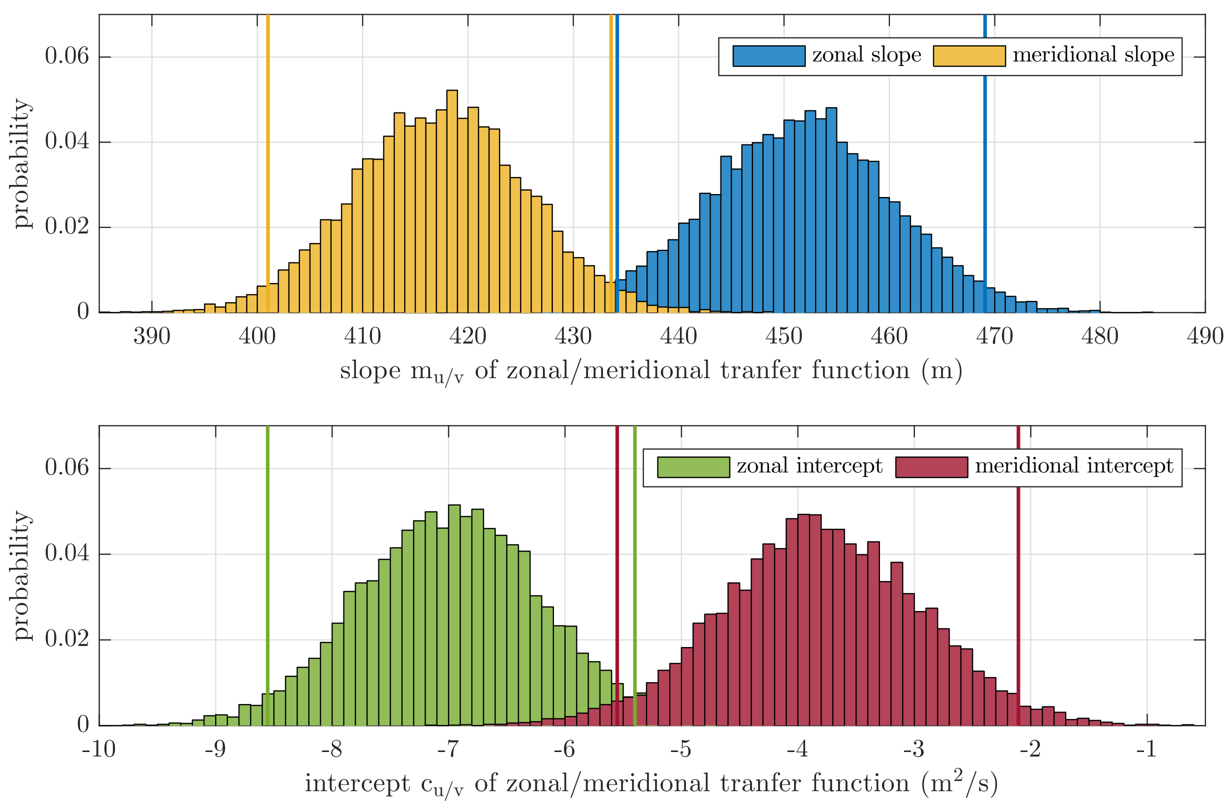

Figure 19: Slope (upper panel) and intercept (lower panel) of the linear transfer function are shown for both zonal and meridional component. The histograms show the normalized distribution of 10000 bootstrap point estimates of each of the 4 parameters. The vertical lines mark the 95 % confidence intervals estimated by the 0.025 and 0.975 quantiles.

3.3.2 Evaluation of the Transfer Function Along 3 Sections

The linear transfer model described here allows for the calculation of surface transports using only the AVISO satellite velocities measured at the surface. The standard error obtained from a bootstrap sampling of the original data provides for an uncertainty estimation of the calculated transports. This model is now tested on the data of the 47°N , MAR and AR7W section described previously. For each of these 3 the ADCP transport is obtained directly from the velocity

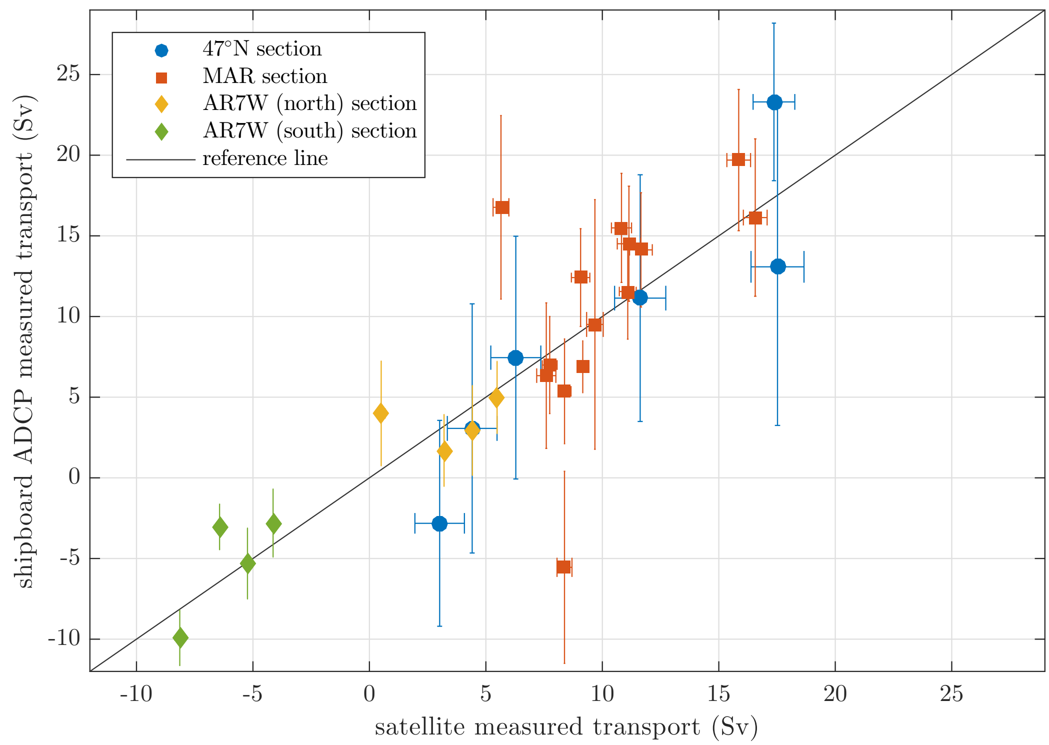

Figure 20: Comparison of surface transports measured by means of ADCP to those calculated from satellite altimetric surface velocities via a linear transfer function. A reference line of slope 1 and intercept 0 is added for orientation. The error bars along the ordinate mark the uncertainty estimate propagated from the 1σ interval in the averaged ADCP velocity measurements, those of the satellite values along the abscissa are based on the variability of the applied transfer function.

profile data along the cruise track. In the case of the 47°N section, the comparison is done for 6 of the 12 cruises that passed it (MSM12/3, MSM21/2, MSM28, MSM38, MSM43, MET85/1). The MAR section has been covered by 7 of the cruises that were analysed (MSM9/1, MSM21/2, MSM28, MSM38, MSM43, MSM53, MET85/1), for each of these there are two transport values since the section was passed twice. The AR7W section was covered by 5 cruises (MSM12/3, MSM28, MSM43, MET85/1, ThalSP), though only by 3 of these to its full extent. The mean flow

Figure 21: Depiction of the geographical position of 3 sections across which transport time series have been calculated from the AVISO velocities. The dots mark the exact locations to which the gridded satellite data have been interpolated.

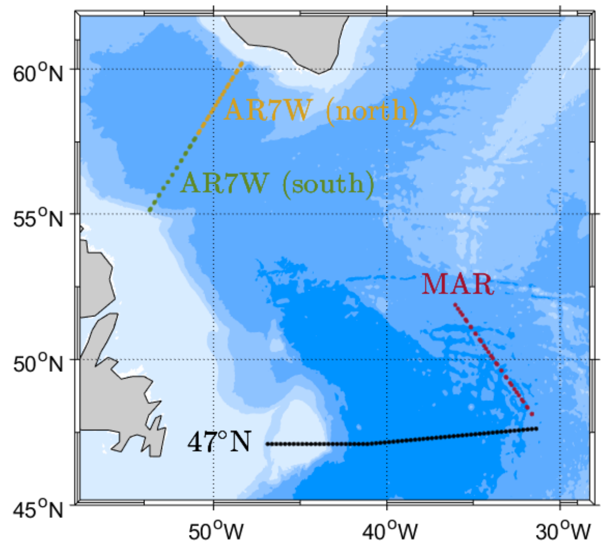

normal to the AR7W section is dominated on the one hand by the West Greenland Current (WGC) flowing to the north-west along the west-coast of Greenland, i.e. into the Labrador Sea and on the other hand by the Labrador Current (LC) flowing to the south-east along Hamilton Bank, i.e. out of the Labrador Sea. The average transport across the entire section will show to be very small compared to the inflow and outflow just described. The section is therefore split at 51.061°W/57.625°N into a northern and a southern part. In the following these two parts will be referred to as *AR7W (north)* and *AR7W (south)*, there are four cruises covering each of the partial sections.

Within the range of their estimated uncertainty the 28 transports inferred from the AVISO velocities compare well to those measured by the ADCP (Fig. 20). However, the uncertainties within the shipboard measurements are very large, ranging from 21 % to over 900 %. These are propagated from the large variance in the velocities – since the ADCP's data is averaged over 2.5 h, the variability of the velocities being averaged is quite high. The rms difference for all 28 measurements pairs is equally high with (4.4 ± 1.1) Sv. Nonetheless the transport measurements still show a high correlation of (84.3 ± 7.1) %. On average the differences largely cancel each other out giving a rather small bias of (0.20 ± 0.91) Sv. Even though the individual deviations are quite high, the averages over the ensemble of all shipboard measured transports on the one hand and all satellite derived transports on the other hand within each respective section differ by only 8.3 % (47°N), 5.0 % (MAR), 1.1 % (AR7W, north) and 13.0 % (AR7W, south).

3.3.3 Transport Time Series Along 3 Sections

Finally the transfer function described above is applied to the daily AVISO data available for the years from 1993 to 2016. The procedure to get time series of surface transports across 3 different sections in the subpolar North Atlantic is very similar to the one used before: The gridded velocity data are interpolated onto the respective section. The resulting velocities are transferred to transports and thereafter the part normal to the section is integrated. Again, this is done for the 3 sections already used in the preceding analysis, namely the 47°N , MAR and AR7W section (Fig. 21). As was the case before the AR7W section is split into a northern and a southern part. To be able to relate the results to the shipboard measurements of transport evaluated above, the extent of the sections that is used now was chosen as a compromise between a good number of cruises having covered the whole section on the one hand and the section remaining as long as possible on the other hand.

The time series of meridional transport across the 47°N section in between 46.875°W and 31.375°W varies around a mean northward transport of (10.2 ± 0.02) Sv within a 1σ interval of (4.3 ± 0.02) Sv (Fig. 22). The northward transport does not exceed (24.0 ± 1.2) Sv. A southward transport across the section is only found 6 times within the 24 years of observation, with the lowest transport being (-5.3 ± 1.1) Sv which occurred on August 4 2014. The variation of the signal is spread over a wide range of time scales from the daily fluctuations in order of 0.1 Sv to oscillations with multi annual period (Fig. 23). Taking the absolute difference between two subsequent transport values as a measure for the daily variability, this can be quantified to be 0.2 Sv. Taking the difference between every second, third and so forth value, the variability increases up to roughly 4 Sv within an interval of 100 d.

The second time series to be evaluated is the transport in north-eastern direction across the section west of the Mid Atlantic Ridge. Its mean amplitude and standard deviation are very similar to that of the 47°N section, being (9.2 ± 0.01) Sv and (4.6 ± 0.01) Sv, respectively. The maximal signal of (24.3 ± 0.6) Sv is also equal to that of the previous section. The two signals, i.e. that of the 47°N and that of the MAR section coincide increasingly when filtered over time. Applying a moving average filter of increasing window length to both time series, the correlation between them increases while the rmsd goes down. This behaviour persists up to

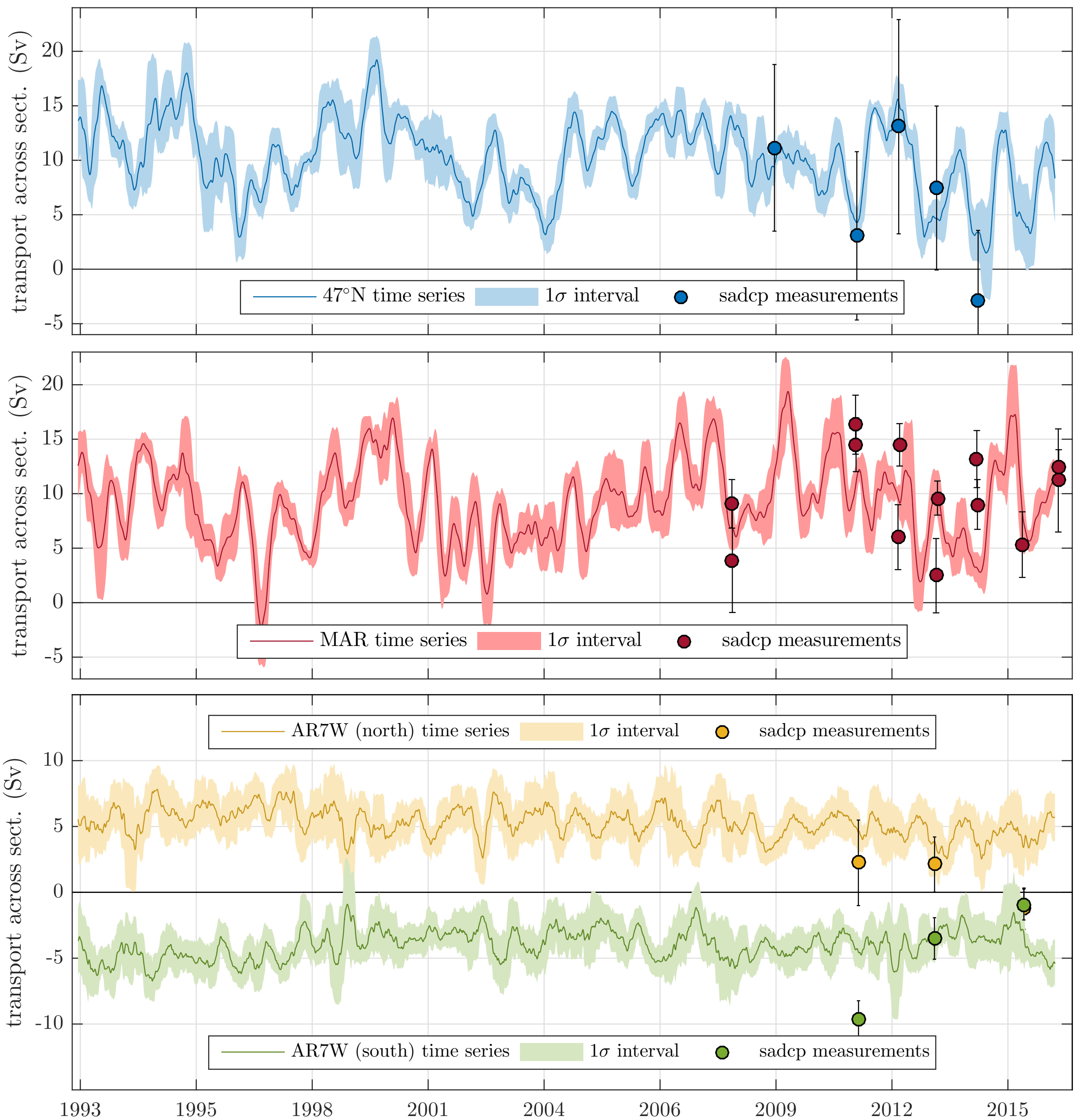

Figure 22: Time series of surface transports inferred from AVISO surface velocity data, compared to single shipboard ADCP measurements. The transports are taken along the 47°N section (upper panel), MAR section (middle panel) and AR7W section (lower panel), respectively. In all three a moving average with a window length of 99 d has been applied to the daily transports. The 1σ interval of the satellite signal corresponds to the standard deviation within the 99 days averaged into one transport value shown here.

time window length of 693 d. For such a running-mean filter applied to the signals, they are correlated by (67.7 ± 2.2) % while the rmsd has dropped to (2.1 ± 0.1) Sv (Fig. 24). A time

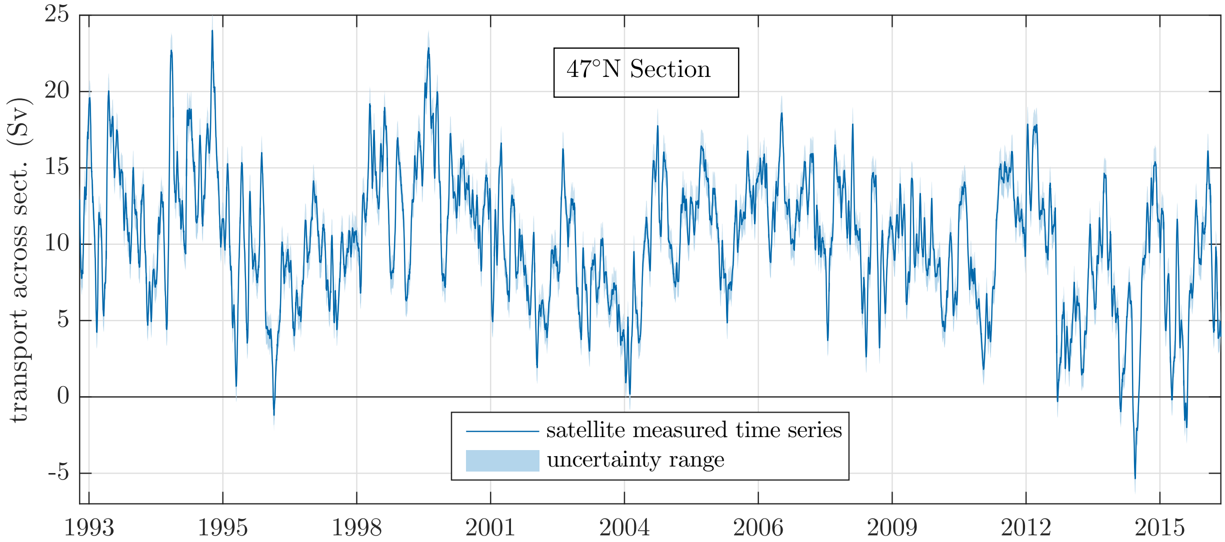

Figure 23: Unfiltered signal of surface transport across the 47°N section as calculated from AVISO velocities. The uncertainty that is hardly visible due to the rapid fluctuation of the signal is based upon the transfer function applied to the velocities.

lag analysis between the filtered time series showed no significant increase of the correlation coefficient. Both sections were reduced on the south-eastern end to further investigate the existence of a time lag relation, i.e. the 47°N section was cut off at 35°W and the MAR section was cut off at 49°N. Repeating the time lag analysis, the correlation coefficient did not increase either. On average the filtered signals differ by (1.1 ± 0.1) Sv, where the transport across the 47°N section is larger. In contrast the unfiltered signals exhibit a significantly smaller correlation of (28.6 ± 0.3) % while at the same time the rmsd of (5.4 ± 0.1) Sv is considerably higher.

The third time series that was looked at is the AR7W, divided into AR7W (north) and AR7W (south). The transports calculated here have a magnitude that is around half of those evaluated so far, ranging around a mean of (5.3 ± 0.01) Sv (north) and (-4.0 ± 0.01) Sv (south). Again the standard deviation is roughly half of the mean signal being (2.2 ± 0.03) Sv for the northern half of the section and (2.1 ± 0.03) Sv for the southern half. The maximal transport directed into the Labrador sea over the northern part of the AR7W is (13.1 ± 0.3) Sv, the maximal transport for the southern part is of comparable size with (-12.3 ± 0.3) Sv, i.e. directed to the south-east. The transports across northern and southern part are negatively correlated with (-55.6 ± 0.2) %. When the signals are filtered with a 693 d moving-average as described above, there is a weak correlation of the AR7W values with the other two transport time series across the 47°N and

MAR section. The highest correlation is found for the transport across the MAR section and the northern half of the AR7W which is (-30.9 ± 4.8) %. Furthermore, the correlation between the 47°N and the AR7W (north) transport is (18.8 ± 4.9) %. There is no significant correlation of the unfiltered AR7W signals with those of the 47°N and MAR section. The residual inflow across the complete AR7W section into the Labrador Sea is simply the sum of its southern and northern part. Hence the mean inflow over the entire section is (1.3 ± 0.01) Sv. This residual transport fluctuates strongly in between maximal values of (-8.0 ± 0.3) Sv and (10.1 ± 0.4) Sv.

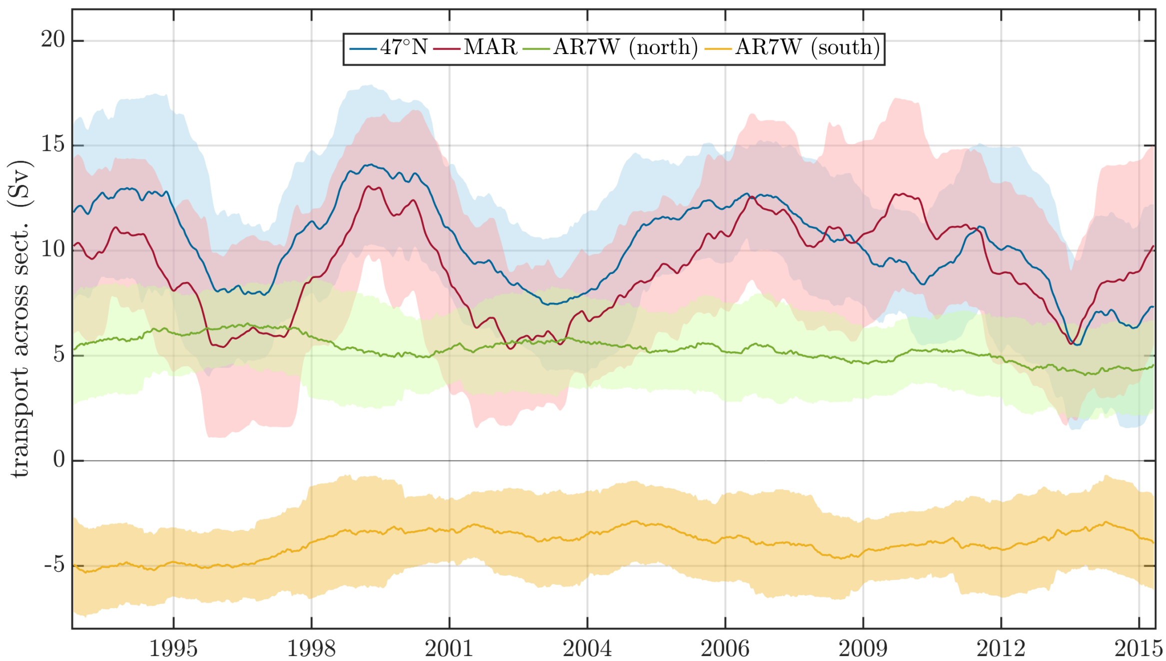

Figure 24: Filtered time series of surface transport across the 47°N , MAR and AR7W section. For all three a moving average filter with a time window length of 693 day has been applied, maximizing the accordance between the 47°N and MAR signal. The shaded area refers to the standard deviation of velocities within the surrounding interval averaged into one transport value.

4. Summary and Discussion

The discussion is divided into 3 parts following the structure in which the results were presented: After a short summary of the preliminary analysis of one cruise's data the main part is going to focus on the statistical analysis of the entire ensemble of velocity measurement pairs. As a last point the transfer of the altimetric velocity data to surface transports as well as the transport time series derived from the altimetry data are to be discussed.

4.1. Evaluation of Averaging Schemes based on the MSM21/2 Data

The starting point of this work was to ask about the fundamental comparability of shipboard in-situ velocity measurements just below the ocean surface and those acquired by remote sensing satellite radar altimetry. A comparison of ADCP data from Cruise Maria S. Merian 21-2 and the absolute geostrophic AVISO velocities already shows that the two instruments provide measurements which differ in the order of magnitude of the signal itself. However, the discordance in terms of absolute deviation is also accompanied by a correlation of the two signals as high as 85.9 % and 88.5 % in the zonal and meridional component, respectively. Both the high absolute differences and the high correlation appear to be tunable by the way in which the shipboard data is processed, yet they remain persistent through all of the tested averaging schemes.

One such parameter that was found to greatly influence the accordance is the time window length of the averaging applied along the cruise track of the ship. In the case of the MSM21/2 cruise, accordance was miximized for an averaging into bins of 2.5 h. Since for the greater part of the cruise the ship is sailing, averaging its data over time necessarily implies that the data is also averaged over distance, more specifically the distance travelled by the ship. The longer the averaging window length gets, the larger the distance covered by the ship becomes. However, the interpolation of the satellite data does not consider spatial widths beyond the size of the AVISO grid. Therefore an averaging window that is too long may result in the comparison of two velocity measurements that are not taken at the same location. This effect is suggested to cause the increasing decorrelation that occurs for averaging window lengths beyond 10 h.

The tidal correction of the ADCP data showed to have no significant influence on the accordance with remotely sensed surface velocities. The differences both in rmsd and in correlation associated with the tidal correction were far below the values' uncertainty estimates and more than 2 orders of magnitude smaller than the mean velocity signal. This is most likely attributable to tidal currents being small in the open ocean – the majority of the data was recorded in waters deeper than 1000 m (Fig. 6)[8].

Three different averaging schemes were applied to the ADCP profiles and yielded a similar but not equal accordance with the AVSIO velocities. Two of these averaged the shipboard data into bins of 2.5 h, one of those in between 22.5 m and 46.5 m, referred to as surface layer, the other one from 46.5 m to 134.5 m, referred to as reference layer. The third scheme averaged into bins of fixed spatial width along the track distance of the ship and over depth within the reference layer. Even though being closer to the surface, the surface layer of the profiles measured by the ADCP shows a greater discordance with the geostrophic surface velocities measured by the satellite. The shallowest bins of an ADCP profile are generally more prone to perturbations by wind induced motion than bins at greater depth. Such perturbations present the most energetic ageostrophic flow near the surface (e.g. Maximenko et al., 2013). Moreover the MSM 21/2 cruise was partly accompanied by strong winds and rough sea. Therefore ageostrophic components in the flow present a plausible hypothesis for the increased discordance close to the surface.

The spatial averaging was thought to be advantageous in scaling the ship's data to the spatial resolution of the altimetric measurements. However, the accordance of both instruments is worse than for an averaging over a constant time. An average over segments of fixed spatial width along the track distance of the ship causes the comprised timespan in each averaged data point to vary. This timespan is smaller than 1 h for more than half of the resulting data. This in turn forces an interpolation of the satellite data to an even smaller spatial and temporal scale than the 2.5 h window used in the other two averaging schemes, which possibly contributes to the deviations.

The above results show how the averaging window length applied to the ADCP data is always a trade off. On the one hand it can't be too long, since the vessel is moving while making the measurements. It is unsurprising that an average of the shipboard data over 100 km does

[8] A description of the theory of ocean tides is given e.g. in Stewart (2008)

not compare well to a satellite observation interpolated to one point. On the other hand the averaging time must not be too short because the resolution of the satellite altimeter is strictly limited. Chelton et al. (2011) investigated the resolution capability of gridded weekly SSH fields provided by AVISO and state the radius of detectable eddies to be about 0.4° or 40 km. Submesoscale processes in the order of 10 km are not resolvable with satellite altimetry (Chavanne and Klein, 2010). (Dufau et al., 2016) are even more pessimistic about the resolution capability of the gridded AVISO maps which they estimate to be around 150-200 km, depending on latitude.

4.2. Comparison of In-Situ ADCP and Satellite Altimetric Velocity Measurements

The main part of this work focusses on the detailed analyses of the entire ensemble of ADCP measurements obtained during 15 different research cruises with largely overlapping cruise tracks in the subpolar North Atlantic, carried out in between 2003 and 2016. The impression gained in the preceding analysis of the MSM21/2 data is carried forward here. A high correlation with the satellite measurements of $(80.4 \pm 0.7)\,\%$ in the zonal and $(84.0 \pm 1.0)\,\%$ in the meridional velocity component goes along with rms deviations of $(10.7 \pm 0.4)\,\mathrm{cm\,s^{-1}}$ and $(11.0 \pm 0.3)\,\mathrm{cm\,s^{-1}}$ in the two respective velocity components, being almost as high as the averaged absolute signal.

The correlation coefficients confirm the results of Ducet et al. (2000) who state that altimetric and in-situ velocities are mainly found to be correlated in between 50 % and 90 %. Ohashi et al. (2013) engaged in a very similar comparison of shipboard ADCP velocities and composite currents from satellite altimetric data, scatterometer measurements providing wind-induced Ekman currents and surface wave-induced Stokes drift as well as model-simulated currents. Moreover, the domain in which they conducted their study is the Northwest Atlantic and hence largely overlaps with the given region. They found the correlation between the altimetric and in-situ velocities to be 59 % with a 95 % confidence interval of $49 - 68\,\%$, which is significantly lower than the results obtained here. However, the large difference may simply be caused by the fact that Ohashi et al. (2013) compared *instantaneous* ADCP observations to those obtained from altimetry, as opposed to the low-passed velocities used in this work. This would be consistent with their assumption that the deviations between the two data sets can be attributed to variability on small spatial and temporal scales. Ohashi et al. (2013)

calculated a bias of $1\,\mathrm{cm\,s^{-1}}$, which is confirmed by the results of this work. They further quantify the accordance between the ADCP observations $\vec{v}_o(t)$ and the composite currents $\vec{v}_c$ by a speed difference ratio SDR $= \left(\sum (\mid \vec{v}_c \mid - \mid \vec{v}_o \mid)^2 / \sum \mid \vec{v}_o \mid^2\right)$ and a vector difference ratio VDR $= \left(\sum (\mid \vec{v}_c - \vec{v}_o \mid)^2 / \sum \mid \vec{v}_o \mid^2\right)$. These are found to be 0.37 in the case of the SDR and 0.61 in the case of the VDR. These measures of absolute deviation are not directly comparable to the rmsd chosen in this work; nonetheless the low SDR and VDR found by Ohashi et al. (2013) are confirmed at least qualitatively by the high rmsd values.

The comparison between Argos-tracked drifters and the AVISO velocities also used in this work that was done by Pascual et al. (2009) found rmsd values of $10.72\,\mathrm{cm\,s^{-1}}$ in the zonal and $9.97\,\mathrm{cm\,s^{-1}}$ in the meridional component, respectively. These values are strikingly close to the rmsd valued found here. Pascual et al. (2009) focused their comparison on energetic zones with large flow velocities outside the equatorial band. While this limitation obviously leaves a vast area remaining which is not covered in this work, it is also one that matches the data given here quite well since the rms of the entire ensemble of ADCP velocity measurements is $19.1\,\mathrm{cm\,s^{-1}}$.

The accordance parameters rmsd, bias and correlation were calculated in order to quantify the accordance between the different instruments' data. They suggest two things which appear to be contradictory at first glance: On the one hand they indicate that both instruments measure significantly different signals. Within their uncertainty range, the rms differences are still almost as high as the actual measurements. This seems plausible, given that the ADCP records local processes at very high resolution both spatially and temporally, while the remote sensing satellite can never register more than the large scale phenomena. Small-scale variability is therefore a reasonable approach towards explaining the discordance, as has been stated before (e.g. Strub et al., 1997). Kelly et al. (1998) found a correlation between the wind-driven Ekman transport and the uncorrelated in-situ velocity, i.e. that part of the in-situ velocity that is uncorrelated with the satellite's signal. As stated earlier, wind-driven ageostrophic components in the flow are another factor that is likely to partly cause the large velocity differences.

On the other hand there is just as strong of an indication that both instrument's signals are not independent of each other, given their high correlation. On the contrary, they rather suggest that the AVISO product used here provides a correct depiction of the flow patterns in the examined region. The dependence between the two velocity ensembles can be described qualitatively by the AVISO velocities being damped with respect to those obtained by the ADCP. This is comprehensible since fluctuations that occur below the spatial or temporal scale visible to the satellite will either not be sampled at all or introduce aliasing errors. The damping is more pronounced in some of the cruises than in others, but nonetheless a recurring pattern that goes along with fast fluctuations of the ADCP signal such as several changes of the flow's heading within one day. Quantitatively this finds expression in the linear relation between both signals. An orthogonal regression showed how the shipboard measured velocity is 1.40-times higher than the one measured by the satellite in the zonal component and 1.20-times higher in the meridional component. The intercept of these regression lines was reassuringly small, being $-2.1\,\mathrm{cm\,s^{-1}}$ and $-0.4\,\mathrm{cm\,s^{-1}}$. The slope parameters that were found to be larger than 1 contradict the work of Boebel and Barron (2003), who found the slope to be 1 at the surface and decrease with depth down to 0.4 below 1000 m. They attribute this to the baroclinic velocity shear (Boebel and Barron, 2003). However, the MODAS-2D velocity fields used by Boebel and Barron (2003) adds climatological SSH fields to the altimeter measurements. Possibly, these enable MODAS not to underestimate the surface currents as much as the AVISO product does.

A further examination of the gap between Satellite and ADCP observations showed how the deviations, when plotted against the mean of both values, show no systematic variation with the respective measurement pair's mean and are centered around zero. Yet this depiction showed once more how large the absolute difference is for a good amount of the data. Zlotnicki et al. (1993) found a spatial dependency of the agreement between in-situ and surface geostrophic velocities obtained with Geosat altimetry in the Cape Verde frontal zone – comparing the data from four moored current meters, the correlation coefficients of the data from the two northernmost moorings was 0.69 and 0.90, while the southernmost moorings gave very low correlations and velocity discrepancies > 100 % (Zlotnicki et al., 1993). In this study the rms deviations were mapped in boxes of 2° across the entire domain and all boxes with less than 5 measurements inside were omitted. The boxes located on the Grand Banks show by far the largest rmsd values reaching up to ca. $30\,\mathrm{cm\,s^{-1}}$. The second notable pattern in the distribution is a patch centred around 40°W/47°N. However, no adequate explanation for the geographic variation of the rmsd could be found – it is further more questionable, in how far these numbers are statistically significant, considering the small number of measurements in many boxes; it is worth mentioning that the rmsd values showed no systematic variation with this number of contributing measurements.

The velocity measurements were then evaluated along the 47°N section in between 47°W and 17°W. Both the data from 12 cruises and the corresponding satellite measurements were interpolated to identical longitudes along the section and subsequently averaged at those query points. Within the ADCP's uncertainty, the meridional components obtained in this way are in complete agreement except for the easternmost 200 km. Likewise, the rmsd values of this averaged section was as low as $(5.0 \pm 0.7)\,\mathrm{cm\,s^{-1}}$ (zonal) and $(4.4 \pm 0.8)\,\mathrm{cm\,s^{-1}}$ (meridional). This agreement is a clear indicator that the differences between single snapshots of velocity are random ones that will vanish for the average of repeated measurements. The standard deviation within the ADCP profiles averaged into one mean value was taken to be an estimator for the shipboard measurement's uncertainty. Considering that in more than 98 % of all ADCP measurements the relative uncertainty derived in this way is larger than 0.1 and in 39 % of all measurements even larger than 1, the described effect should not be too surprising. The shipboard observations as they were used here still present an average over a significant stretch of time and space. How well this compares to one individual point measurement is obviously subject to a good amount of coincidence. Yet in the mean these random fluctuations become insignificant which yields the striking similarity of the averaged velocity sections.

4.3. Transferring Satellite Velocities to Surface Transports

The volumetric transport within the upper ocean layer in between 50 m and 550 m was calculated from the ADCP measurements. Due to the application of the temporal averaging the horizontal distance contributing to one averaged ADCP observation varies for each point, these transports were calculated per unit horizontal distance ($\mathrm{m^2 s^{-1}}$). The empirical linear relation of the transports and the co-located altimetric velocity measurements was taken to be a transfer function between the two quantities:

$$U_{\mathrm{ACDP}} = (451.5 \pm 8.8)\,\mathrm{m} \cdot u_{\mathrm{sat}} - (7.0 \pm 0.8)\,\mathrm{m^2/s} \tag{18}$$

$$V_{\mathrm{ACDP}} = (417.5 \pm 8.2)\,\mathrm{m} \cdot v_{\mathrm{sat}} - (3.8 \pm 0.9)\,\mathrm{m^2/s} \tag{19}$$

The standard errors of the slope and intercept parameters $(m_{\mathrm{u}}, c_{\mathrm{u}}, m_{\mathrm{v}}, c_{\mathrm{v}})$ were calculated from the distribution of 10000 bootstrap resamples of the actual data. For an evaluation of the set of transfer functions given in Eqn. 19 the volumetric transport across 3 different section in the

SPNA was calculated on the one hand from the AVISO velocities via this particular function and on the other hand from the ADCP measurements, taking the latter of the two to be a benchmark for the actual transport. This comparison yielded 28 individual transport values, 6 of which come from the 47°N section, 14 from the MAR section and 4 from the AR7W (north) and AR7W (south) section, respectively. These values range from $-11.0\,$Sv to 23.3 Sv around a mean 7.1 Sv. The rmsd of all 25 observation pairs is $(4.4 \pm 1.1)\,$Sv, which corresponds to more than 50 % of their mean. Carrying forward the pattern already notable in the comparison of velocities, the correlation of $(84.3 \pm 7.1)\,$% between all 28 measurement pairs is rather high. When averaged within one section, shipboard measured and altimetric transports differ by only 8.3 % (47°N), 5.0 % (MAR), 1.1 % (AR7W, north) and 13.0 % (AR7W, south).

As stated before, the large uncertainty within the transport values derived from the ADCP profiles is propagated from the velocities' uncertainty estimates. What happens in detail is that the high resolution profiles are averaged along the section to produce the filtered velocities that were compared to the AVISO data. The standard deviation of these was then termed *error estimate*. While this method surely prevents an overly optimistic estimate of the accuracy of the transport values, it is all the same misguiding in the opposite direction – since the transport will be constituted by the velocity at every point along the section, the variability within one interval of 2.5 h along the cruise track does not affect the accuracy of the shipboard measured transport. Therefore one should be very cautious in attributing the large difference between AVISO derived and ADCP measured transports to the given ADCP uncertainties.

What appears to be a more promising approach to explaining the large absolute deviation is to focus on the transfer function. It is based purely on the high correlation between satellite measured velocities and shipboard measured transports. But all this correlation coefficient states is that *on average* the 3269 measurement pairs lead to the linear relation that was used. The individual realisation may depart significantly from this simple model, which is put into numbers by the large 95 % confidence interval of the slope and intercept parameters. While the range of this interval is quite small for the *slope* parameters, being 7.6 % of the slope in both velocity components, is is all the large for the *intercept* parameters. The confidence interval ranges over 44.3 % of the intercept value in the zonal and 89.5 % in the meridional component, respectively. Associating the transport differences with the inaccuracy of the transfer function would be consistent with the fact that on average the multiple transport observations derived from the in-situ and the altimetric data are very close for all 4 sections, with relative differences moving in between 1.1 % and 13.0 %.

The transport time series that were calculated from the AVSIO data should equally be evaluated against this backdrop. While the daily values may be unreliable in the light of the named deviations, averaging these over a sufficient number of days should provide for accurate estimates of e.g. monthly means of the upper ocean transport. Keeping this in mind, it was possible to transfer the satellite altimetric velocity fields into time series of transport across the 3 sections that were named.

The time series across the 47°N section is characterized by the largest transports of all three sections. The mean northward transport within the upper 500 m and in between 46.875°W and 31.375°W was found to be (10.2 ± 0.02) Sv with a standard deviation of 4.3 Sv. There is numerous measurements of the absolute transport across the 47°N sections, as summarized by (Rhein et al., 2011). A direct comparison with these is not feasible in most cases since the transports calculated here are restricted to depths of 50 m to 550 m. Mertens et al. (2014) studied the circulation east of Flemish Cap by seven repeat hydrographic sections along the 47°N in the time period from 2003 to 2011. They estimate the mean northward transport sustained by the NAC to be (111.9 ± 20.5) Sv of which (77.6 ± 13.7) Sv recirculate southward east of the NAC. They find a persistence of a strong northward NAC and a slightly weaker recirculation east of the NAC core in all averaged measurements which is confirmed by this works findings – the long term average of the net transport across the 47°N section is solely positive.

The transport across the section west of the Mid-Atlantic Ridge in north-eastern direction was found to be (9.2 ± 0.01) Sv in the SI24year mean, i.e. 1 Sv lower than the net transport of water across the zonal section at 47°N . Those two transport time series with a daily temporal resolution are correlated by (28.6 ± 0.3) %. When filtered with a moving average of a window length of 693 days, the 47°N and MAR transport data exhibit a much higher correlation of (67.7 ± 2.2) %, showing how the two signals are connected on a multi annual timescale. This confirms the MAR section parallel to the Mid Atlantic Ridge as a main pathway of the NAC to the north-east, as stated e.g. by (Bower et al., 2002).

An approach very similar to the one chosen in this work was used by Roessler et al. (2015) to calculate a time series of NAC transports across the MAR section in between 47.667°N and 52.500°N for the period from 1992 to 2013. They made use of the correlation between transport observations obtained from four moored inverted echo sounders with high precision pressure sensors in between 2006 and 2010 and geostrophic velocity measurements from altimeter data to extend the transport time series to the period for which the altimeter derived velocities were available. Since their findings refer to the entire water column, they are comparable to this work's finding qualitatively. Their total mean NAC transport for the entire period of 1992 to 2013 is 27.5 Sv with a standard deviation of 4.6 Sv. Considering that oceanic velocities generally tend to decrease with depth, this transport would be compatible with the 9.2 Sv found here. Within its precision of 0.1 Sv their standard deviation matches the one that was found here exactly. Roessler et al. (2015) found individual observations that were less than 14 Sv to over 40 Sv which resembles a comparably large range as the one encountered in this work. Their annual means fluctuate in between 20 Sv and 31 Sv and show a very similar regime as the 693 d filtered transport in this work – the longterm local maxima and minima of the time series match the ones found here. It is consistent that both their annual means and the individual transports exhibit a behaviour that is very similar to the MAR transport time series in this work since both are based on the same altimeter observations.

Another study that looked at the eastward flow across a slightly different section west of the MAR located at 36°W between 47° and 53°N found the 2 year mean transport in the layer above 1000 dbar to be 21 Sv (Perez-Brunius et al., 2004). Their work applies a technique called float-Gravest Empirical Mode (float-GEM)[9] to 2 isopycnal RAFOS float experiments from 1993 to 2000, mapping mean absolute mass transports in an area bounded by 40°N, 55°N, 55°W and 25°W to the south, north, east and west, respectively. Their mean transport value is about 2.3 times higher than the one found here while referring to about twice the depth and a slightly larger latitudinal extent of the section. Without information about the mean velocity shear a quanti-

[9]float-GEM was developed by Perez-Brunius et al. (2004). It combines pressure measurements from isopycnal floats and historical hydrography to obtain mean three-dimensional temperature and density fields and consequently also the baroclinic velocity field. It estimates absolute velocity fields as well as volume and temperature transports via the floats' velocity measurements (Perez-Brunius et al., 2004).

tative comparison cannot be made, nonetheless the transport values do not contradict each other.

Breckenfelder et al. (2017) compare observational transport time series across the MAR section to the output of a high-resolution model. Amongst others, they make use of CTD (conductivity, temperature and pressure sensor) and lowered ADCP measurements from 7 hydrographic sections along the MAR section in between 2008 and 2015. They found the observed baroclinic mean transport relative to 3400 m to be (27.4 ± 4.7) Sv. Just as before, their estimate of the mean transport is compatible with the 9.2 Sv found for the upper 500 m. The lowered ADCP measurements used by Breckenfelder et al. (2017) were made available for a direct comparison of the mean 50 to 550 m transport which was found to be (10.0 ± 4.7) Sv, confirming the findings of this work.

The transport time series across the AR7W section provided information both about the mean inflow of the WGC, which was found to be (5.3 ± 0.01) Sv in the upper 500 m that were investigated, and about the mean outflow of the LC which was found to be (-4.0 ± 0.01) Sv, i.e. directed out of the Labrador Sea. There was little correlation between the AR7W transports with those of the 47°N and the MAR section. However, the northern and southern part of the section are correlated negatively by (-55.6 ± 0.2) % which indicates that the strength of the LC is largely constituted by the strength of the inflow into the Labrador Sea. The residual transport which is the sum of northern and southern transport is (1.3 ± 0.01) Sv on average. The section that was analysed here ends at 53.677°W/55.125°N in the south-west. Hall et al. (2013) analysed six lowered ADCP sections along the AR7W section in between 1995 and 2008 to determine the absolute velocity across the section. They construct a composite velocity field that averages the six sections and shows that there is substantial southward transport taking place beyond the point where this work's section ends. While this might be the reason for the residual northward transport across the entire section, there is also northward transport beyond the northern end of the section used here. Another possibility would be that the velocity shear of the north-eastern boundary current is stronger than that of the south-western. Hall et al. (2013) furthermore found a bottom current in the middle of the AR7W section. While this definitely supports southward export of water from the Labrador sea, it seems unlikely to cause a residual inflow at the surface that is almost 25 % of the total inflow across the section.

Hall et al. (2013) also state the flow to be *virtually uniform* in depth in the interior of the section. The velocities of the cyclonic boundary current system do decrease with depth but are still in the order of $15\,\mathrm{cm\,s^{-1}}$ at the bottom. The existence of top-to-bottom bands of velocity backs up the approach chosen in this work since it makes the connection between surface velocity and transport below the surface feasible.

5. Conclusions and Outlook

This work was concerned to evaluate in how far the ocean surface velocity measurements derived from satellite radar altimetric SSH measurements are comparable to in-situ velocity observations made with shipboard ADCP in the subpolar North Atlantic. Two main statements can be drawn from the statistical analysis with high confidence. The satellite altimetric measurements are highly correlated to those recorded by the ADCP, with correlation coefficients of the entire ensemble of measurements being greater than 80% in both velocity components. While these numbers suggest a good accordance of the two measurement techniques, the absolute deviations expressed in terms of rmsd are also very high, being around $11\,\mathrm{cm\,s^{-1}}$ in both the zonal and the meridional component. These numbers are in good agreement with preceding findings as layed out in detail within the discussion.

Two ways of reading the high rmsd numbers are promoted: On the one hand there is a methodological limitation to a comparison of under way measurements to those taken by means of remote sensing satellites. A filtering of the in-situ data is inevitable if one wishes to omit features associated with small scale variability; however, averaging the data collected by a moving vessel will always result in the summation of measurements taken along a significant extent of space and time. On the other hand, there is a large gap in what is physically observable for the two instruments; at least parts of the large rms deviations are very likely to be attributable to ageostrophic components in the flow.

The transfer function which connects the AVISO velocities to shipboard transport measurements allows for the calculation of volumetric transport in the upper ocean layer. The correlation between the ADCP transport measurements and those obtained indirectly from satellite altimetric velocities is very high while the absolute deviation of transport measurements along selected sections in the SPNA is equally very high.

The conclusion drawn from the statistical analysis is the same for both the comparison of velocities and the comparison of transports. The significantly increased accordance of averaged measurements suggests that the absolute discordances are generally random and do not contradict the high correlations. In the case of the comparison of velocities this was shown for the averaging of repeated measurements along the 47°N section. The transports were compared along the 47°N , MAR and AR7W section and all three of them exhibit the described behaviour.

Thus, while the individual measurements' rmsd is too high to infer precise information about the subsurface flow from one single satellite measurement, there is much less uncertainty in a set of averaged independent observations. This clearly indicates the usefulness of the suggested transfer function for the analysis of monthly averages, seasonal patterns or multi-annual variation.

A question that is left unanswered by this work is how many satellite measurements one needs to obtain a certain amount of precision for the averaged transport estimate. To answer this question one would need to compare a larger amount of transport measurements and analyse the accordance of in-situ and satellite estimates with respect to the number of contributing measurements. This was not feasible here, considering the 28 transport observations from 3 different sections that were available from the ADCP data.

Another open question is why the linear relation between ADCP measured transport and satellite measured surface velocity yields a slightly different transfer function for the zonal and meridional component. Within the scope of this work no explanation could be found.

A. Abbreviations

ADCP acoustic Doppler current profiler

ADT absolute dynamic topography

AVISO Archiving, Validation and Interpretation of Satellite Oceanographic data

float-GEM float-Gravest Empirical Mode

LC Labrador Current

MDT mean dynamic topography

MSS mean sea surface

NAC North Atlantic Current

OLS ordinary least squares regression

PG *percent good* parameter

rms root-mean-square

rmsd root-mean-square deviation

SDR speed difference ratio

SLA sea level anomaly

SPNA subpolar North Atlantic

SSH sea surface height

VDR vector difference ratio

WGC West Greenland Current

B. Nomenclature

α angle between transducer- and scatterer velocity

c speed of sound

Δf observed change in frequency

$\partial p/\partial x$ horizontal pressure gradient (zonal)

$\partial p/\partial y$ horizontal pressure gradient (meridional)

η gradient of sea surface height

f Coriolis parameter

f_0 emitted frequency

f_1 observed frequency

g gravitational acceleration

Ω period of Earth's rotation about its own axis

ϕ latitude

R range (distance between satellite and Earth surface)

ρ density of seawater

S satellite's heigh above the reference ellipsoid

$u_{\mathbf{g}}$ geostrophic velocity (zonal)

$v_{\mathbf{g}}$ geostrophic velocity (meridional)

$v_{\mathbf{r}}$ velocity of receiver (relative to medium)

$v_{\mathbf{s}}$ velocity of source (relative to medium)

C. List of Cruises

MET59/1 Meteor 59/1 (June-July 2003)

MET59/2 Meteor 59/2 (July-August 2003)

MET85/1 Meteor 85/1 (June-August 2011)

MSM12/3 M.S.Merian 12/3 (July-August 2009)

MSM21/2 M.S.Merian 21/2 (June-July 2012)

MSM27 M.S.Merian 27 (April-May 2013)

MSM28 M.S.Merian 28 (May-June 2013)

MSM38 M.S.Merian 38 (May-June 2014)

MSM39 M.S.Merian 39 (June-July 2014)

MSM42 M.S.Merian 42 (May 2015)

MSM43 M.S.Merian 43 (May-June 2015)

MSM5/1 M.S.Merian 5/1 (April-May 2007)

MSM53 M.S.Merian 53 (March-May 2016)

MSM9/1 M.S.Merian 9/1 (July-August 2008)

ThalSP Thalassa SPOL (June-July 2005)

D. References

Arbic, B. K., R. Scott, D. Chelton, J. Richman, and J. Shriver, 2012: Effects of stencil width on surface ocean geostrophic velocity and vorticity estimation from gridded satellite altimeter data. *Journal of Geophysical Research: Oceans*, **117 (C3)**, n/a–n/a, doi:10.1029/2011JC007367.

Birol, F., J. Brankart, J. Lemoine, P. Brasseur, and J. Verron, 2005: Assimilation of satellite altimetry referenced to the new grace geoid estimate. *Geophysical Research Letters*, **32 (6)**, doi:10.1029/2004GL021329.

Boebel, O., and C. Barron, 2003: A comparison of in-situ float velocities with altimeter derived geostrophic velocities. *Deep Sea Research Part II: Topical Studies in Oceanography*, **50 (1)**, 119 – 139, doi:http://dx.doi.org/10.1016/S0967-0645(02)00381-8.

Bower, A., and Coauthors, 2002: Directly measured mid-depth circulation in the northeastern north atlantic ocean. *Nature*, **419 (6907)**, 603–607, doi:10.1038/nature01078.

Breckenfelder, T., M. Rhein, A. Roessler, C. W. Boening, A. Biastoch, E. Behrens, and C. Mertens, 2017: Flow paths and variability of the north atlantic current: A comparison of observations and a high-resolution model. *Journal of Geophysical Research-Oceans*, **122 (4)**, 2686–2708, doi: 10.1002/2016JC012444.

Chang, C.-H., C.-Y. Kuo, C. Shum, Y. Yi, and A. Rateb, 2016: Global surface and subsurface geostrophic currents from multi-mission satellite altimetry and hydrographic data, 1996-2011. *Journal of marine science and technology - Taiwan*, **24 (6)**, 1181–1193, doi: 10.6119/JMST-016-1026-7.

Chavanne, C. P., and P. Klein, 2010: Can oceanic submesoscale processes be observed with satellite altimetry? *Geophysical Research Letters*, **37**, doi:10.1029/2010GL045057.

Chelton, D. B., M. G. Schlax, and R. M. Samelson, 2011: Global observations of nonlinear mesoscale eddies. *Progress in Oceanography*, **91 (2)**, 167 – 216, doi:http://dx.doi.org/10.1016/j.pocean.2011.01.002.

Ducet, N., P.-Y. L. Traon, and G. Reverdin, 2000: Global high-resolution mapping of ocean circulation from topex/poseidon and ers-1 and -2. *Journal of Geophysical Research: Oceans*, **105 (C8)**, 19 477–19 498, doi:10.1029/2000JC900063.

Dufau, C., M. Orsztynowicz, G. Dibarboure, R. Morrow, and P.-Y. L. Traon, 2016: Mesoscale resolution capability of altimetry: Present and future. *Journal of Geophysical Research - Oceans*, **121 (7)**, 4910–4927, doi:10.1002/2015JC010904.

Egbert, G., and M. F. A.F. Bennett, 1994: Topex/poseidon tides estimated using a global inverse model. *Journal of Geophysical Research: Oceans*, **99 (C12)**, 24 821–24 852, doi:10.1029/94JC01894.

Egbert, G., and S. Erofeeva, 2002: Efficient inverse modeling of barotropic ocean tides. *Journal of Atmospheric and Oceanic Technology*, **19 (2)**, 183–204, doi:10.1175/1520-0426(2002)019<0183:EIMOBO>2.0.CO;2.

Fratantoni, D., 2001: North atlantic surface circulation during the 1990's observed with satellite-tracked drifters. *Journal of Geophysical Research-Oceans*, **106 (C10)**, 22 067–22 093, doi:10.1029/2000JC000730.

Hall, M. M., D. J. Torres, and I. Yashayaev, 2013: Absolute velocity along the ar7w section in the labrador sea. *DEEP-SEA RESEARCH PART I-OCEANOGRAPHIC RESEARCH PAPERS*, **72**, 72–87, doi:10.1016/j.dsr.2012.11.005.

Helland-Hansen, B., and F. Nansen, 1920: Temperature variations in the north atlantic ocean and in the atmosphere. *Smithsonian miscellaneous collections*, **70 (4)**, 408 pp.

Hummon, J., and E. Firing, 2003: A direct comparison of two rdi shipboard adcps: A 75-khz ocean surveyor and a 150-khz narrow band. *Journal of Atmospheric and Oceaning Technology*, **20 (6)**, 872–888, doi:10.1175/1520-0426(2003)020<0872:ADCOTR>2.0.CO;2.

Kelly, K. A., R. Beardsley, R. Limeburner, K. Brink, J. Paduan, and T. Chereskin, 1998: Variability of the near-surface eddy kinetic energy in the california current based on altimetric, drifter, and moored current data. *Journal of Geophysical Research: Oceans*, **103 (C6)**, 13 067–13 083, doi:10.1029/97JC03760.

Le Traon, P. Y., 2013: From satellite altimetry to argo and operational oceanography: three revolutions in oceanography. *Ocean Science*, **9 (5)**, 901–915, doi:10.5194/os-9-901-2013.

Maximenko, N., R. Lumpkin, and L. Centurioni, 2013: Ocean surface circulation. *International Geophysics*, **103**, 283 – 304, doi:http://dx.doi.org/10.1016/B978-0-12-391851-2.00012-X.

Maximenko, N., P. Niiler, L. Centurioni, M.-H. Rio, O. Melnichenko, D. Chambers, V. Zlotnicki, and B. Galperin, 2009: Mean dynamic topography of the ocean derived from satellite and drifting buoy data using three different techniques. *Journal of Atmospheric and Oceanic Technology*, **26 (9)**, 1910–1919, doi:10.1175/2009JTECHO672.1.

Mertens, C., M. Rhein, M. Walter, C. W. Böning, E. Behrens, D. Kieke, R. Steinfeldt, and U. Stöber, 2014: Circulation and transports in the newfoundland basin, western subpolar north atlantic. *Journal of Geophysical Research: Oceans*, **119 (11)**, 7772–7793, doi:10.1002/2014JC010019.

Munk, W., 2000: Chapter 1 oceanography before, and after, the advent of satellites. *Elsevier Oceanography Series*, **63**, 1 – 4, doi:http://dx.doi.org/10.1016/S0422-9894(00)80002-1, satellites, oceanograghy and society.

Ohashi, K., G. Han, N. Chen, and J. Helbig, 2013: Northwest atlantic surface circulation from multi-satellite observations. *Atmosphere-Ocean*, **51 (1)**, 35–49, doi:10.1080/07055900.2012.747951, URL http://dx.doi.org/10.1080/07055900.2012.747951.

Pascual, A., C. Boone, G. Larnicol, and P.-Y. L. Traon, 2009: On the quality of real-time altimeter gridded fields: Comparison with in situ data. *Journal of Atmospheric and Oceanic Technology*, **26 (3)**, 556–569, doi:10.1175/2008JTECHO556.1.

Perez-Brunius, P., T. Rossby, and D. Watts, 2004: Absolute transports of mass and temperature for the north atlantic current-subpolar front system. *Journal of Physical Oceanography*, **34 (8)**, 1870–1883, doi:{10.1175/1520-0485(2004)034<1870:ATOMAT>2.0.CO;2}.

Perez-Brunius, P., T. Rossby, and D. Watts, 2004: A method for obtaining the mean transports of ocean currents by combining isopycnal float data with historical hydrography. *Journal of Atmospheric and Oceanic Technology*, **21 (2)**, 298–316, doi:10.1175/1520-0426(2004)021<0298:AMFOTM>2.0.CO;2.

Picaut, J., A. Busalacchi, M. McPhaden, and B. Camusat, 1990: Validation of the geostrophic method for estimating zonal currents at the equator from geosat altimeter data. *Journa of Geophysical Research - Oceans*, **95 (C3)**, 3015–3024, doi:10.1029/JC095iC03p03015.

Rhein, M., and Coauthors, 2011: Deep water formation, the subpolar gyre, and the meridional overturning circulation in the subpolar north atlantic. *Deep Sea Research Part II: Topical Studies in Oceanography*, **58 (17-18)**, 1819 – 1832, doi:https://doi.org/10.1016/j.dsr2.2010.10.061.

Rio, M., and F. Hernandez, 2004: A mean dynamic topography computed over the world ocean from altimetry, in situ measurements, and a geoid model. *Journal of Geophysical Reasearch-Oceans*, **109 (C12)**, doi:10.1029/2003JC002226.

Rio, M. H., S. Mulet, E. Greiner, N. Picot, and A. Pascual, 2013: New global mean dynamic topography from a goce geoid model, altimeter measurements and oceanographic in-situ data. Ocean Surface Topography Science Team Meeting and 7th Coastal Altimetry Workshop, Boulder, Colorado, U.S.A., 8-11 October.

Roessler, A., M. Rhein, D. Kieke, and C. Mertens, 2015: Long-term observations of north atlantic current transport at the gateway between western and eastern atlantic. *Journal of Geophysical Research: Oceans*, **120**, 4003–4027, doi:10.1002/2014JC010662.

SSALTO/Duacs new product version, 2014, 2014: A new version of ssalto/duacs products available in april 2014, issue 1.0.

SSALTO/Duacs User Handbook, 2016, 2016: Ssalto/duacs user handbook: Msla and (m)adt near-real time and delayed time products. URL http://www.aviso.oceanobs.com/fileadmin/documents/data/tools/hdbk$_$duacs.pdf, cLS-DOS-NT-06-034. Issue 5.0. Nomenclature: SALP-MU-P-EA-21065-CLS.

Stewart, R., 2008: *Introduction to physical oceanography*. Prentice Hall, Editor: University, Texas A M, doi:10.1119/1.18716.

Strub, P. T., P. N. T.K. Chereskin, C. James, and M. Levine, 1997: Altimeter-derived variability of surface velocities in the california current system: 1. evaluation of topex altimeter velocity resolution. *Journal of Geophysical Research: Oceans*, **102 (C6)**, 12 727–12 748, doi:10.1029/97JC00448.

Talley, L. D., G. Pickard, W. Emery, and J. Swift, 2011: Chapter {S16} - instruments and methods. *Descriptive Physical Oceanography (Sixth Edition)*, L. D. Talley, G. L. Pickard, W. J. Emery, and J. H. Swift, Eds., sixth edition ed., Academic Press, Boston, 1 – 83, doi:https://doi.org/10.1016/B978-0-7506-4552-2.10028-9.

Tapley, B., S. Bettadpur, M. Watkins, and C. Reigber, 2004: The gravity recovery and climate experiment: Mission overview and early results. *Geophysical Research Letters*, **31 (9)**, doi:10.1029/2004GL019920.

Tapley, B., D. Chambers, S. Bettadpur, and J. Ries, 2003: Large scale ocean circulation from the grace ggm01 geoid. *Geophysical Research Letters*, **30 (22)**, doi:10.1029/2003GL018622.

TRD Broadband Primer (2006), 2006: Acoustic doppler current profiler – principles of operation – a practical primer, third edition for broadband adcps. 2006 by Teledyne RD Instruments.

Thomson, R. E., and W. Emery, 2014: Chapter 1 - data acquisition and recording. *Data Analysis Methods in Physical Oceanography (Third Edition)*, W. J. Emery, and R. E. Thomson, Eds., third edition ed., Elsevier, Boston, doi:https://doi.org/10.1016/B978-0-12-387782-6.00004-1.

Traon, P.-Y. L., and Coauthors, 2015: Use of satellite observations for operational oceanography: recent achievements and future prospects. *Journal of Operational Oceanography*, **8 (sup1)**, s12–s27, doi:10.1080/1755876X.2015.1022050.

U.S. Department of Commerce, 2001, 2001: Global gridded 2-minute database, natl. oceanic and atmos. admin. natl. geophys. data cent. (ngdc), boulder, colo. URL http://www.ngdc.noaa.gov/mgg/global/etopo2.html.

Wehrens, R., H. Putter, and L. Buydens, 2000: The bootstrap: a tutorial. *Chemometrics and Intelligent Laboratory Systems*, **54 (1)**, 35 – 52, doi:http://dx.doi.org/10.1016/S0169-7439(00)00102-7.

Wunsch, C., and E. Gaposchkin, 1980: On using satellite altimetry to determine the general circuation of the oceans with application to geoid improvement. *Reviwes of Geophysics*, **18 (4)**, 725–745, doi:10.1029/RG018i004p00725.

Wunsch, C., and D. Stammer, 1998: Satellite altimetry, the marine geoid, and the oceanic general circulation. *Annual Review of Earth and Planetary Sciences*, **26**, 219–253, doi:10.1146/annurev.earth.26.1.219.

Xu, S., 2014: A property of geometric mean regression. *American Statistician*, **68 (4)**, 277–281, doi:10.1080/00031305.2014.962763.

Yu, Y., W. Emery, and R. Leben, 1995: Satellite altimeter derived geostrophic currents in the western tropical pacific during 1992-1993 and their validation with drifting buoy trajectories. *Journal of Geophysical Research: Oceans*, **100 (C12)**, 25 069–25 085, doi:10.1029/95JC02146.

Zlotnicki, V., G. Siedler, and B. Klein, 1993: Can the weak surface currents of the cape verde frontal zone be measured with altimetry? *Journal of Geophysical Research: Oceans*, **98 (C2)**, 2485–2493, doi:10.1029/92JC02729.

E. Urheberrechtliche Erklärung

Nachname: Cordts

Vorname: Robert

Matrikelnr. 2991929

Hiermit versichere ich, dass ich die vorliegende Arbeit selbstständig verfasst und keine anderen als die angegebenen Quellen und Hilfsmittel verwendet habe. Alle Stellen, die ich wörtlich oder sinngemäß aus anderen Werken entnommen habe, habe ich unter Angabe der Quellen als solche kenntlich gemacht.

Ort, Datum Unterschrift

F. Erklärung zur Veröffentlichung von Abschlussarbeiten

Ich bin damit einverstanden, dass meine Abschlussarbeit im Universitätsarchiv für wissenschaftliche Zwecke von Dritten eingesehen werden darf.

Ort, Datum Unterschrift

G. Acknowledgements

First and foremost I would like to thank Christian Mertens for his helpful advice on thesis writing, his valuable ideas for this work, the willingness for discussion and the proof-reading that made up his supervision.

I want to give thanks to Torsten Kanzow for evaluating my thesis as second examiner.

Furthermore, I would like to thank the members of the Physical Oceanography working group of the University of Bremen who were always available to discuss and answer my questions whenever I would walk into their office.

Finally I would like to thank my fellow students for their support, advice and time for coffee breaks.